

A STUDY OF A REINFORCED CONCRETE
SKEW GRILLAGE BRIDGE UNDER ULTIMATE LOAD

A Thesis
Presented to
the Faculty of Graduate Studies
The University of Manitoba

In Partial Fulfillment
of the Requirements for the Degree
Master of Science

by
Kularb Narong
February, 1970



TABLE OF CONTENTS

	<u>Page</u>
ABSTRACT	iv
ACKNOWLEDGMENT	v
LIST OF TABLES	vi
LIST OF FIGURES	vii
LIST OF PHOTOGRAPHS	viii
NOTATION	x
 <u>CHAPTER</u>	
I. INTRODUCTION AND REVIEW	1
1.1 Introduction	1
1.2 Review of Elastic and Plastic Theories	2
1.3 Object of the Test	4
1.4 Historical Bibliography	6
II. DESIGN OF A SKEW GRILLAGE BRIDGE	8
2.1 General Considerations	8
2.2 Description of the Skew Grillage Bridge	8
2.3 Scale Relations	10
2.4 Design of the Model	11
2.5 Determination of the Ultimate Load for the Model	15
III. SPECIMEN AND TESTING APPARATUS	18
3.1 Model Construction	18
3.2 Materials Properties	21
3.3 Testing Apparatus	27

TABLE OF CONTENTS (CONTINUED)

<u>CHAPTER</u>	<u>Page</u>
IV. TEST OF THE MODEL AND RESULTS	29
4.1 Testing Procedure	29
4.2 Results of the Test	30
V. CONCLUSIONS AND SUGGESTIONS FOR FURTHER RESEARCH	42
5.1 Conclusions	42
5.2 Suggestions for Further Study	44
BIBIOGRAPHY	46
APPENDIX A. CALCULATION OF PLASTIC BENDING STRENGTHS AND TORSIONAL STRENGTHS IN BEAMS	48
APPENDIX B. CALCULATION OF THE ULTIMATE LOAD FOR THE MODEL	55
APPENDIX C. TABLES OF LOAD-DEFLECTION READINGS	60

Abstract

A laboratory test was made on a one-fourth scale simply-supported, reinforced concrete grillage bridge having a skew angle of 30 degrees. The model structure was chosen to accommodate a 2-lane capacity and was designed for H20 - S16 highway truck loading. The design was based on the elastic theory but the structure was analyzed for collapse strength by the yield hinge theory. In this particular test it was assumed that the critical condition prevailed; that is, four equal wheel loads applied at the same time to the four middle node points. The predicted ultimate wheel load was obtained by using the method of upper and lower bounds.

The purposes of the test were:

- (i) To determine the ultimate capacity of the skew grillage bridge;
- (ii) To observe conditions at the ultimate load - in particular, how the concrete cracked and was crushed and to measure the maximum deflection when the reinforcing first yielded.

The result of the test showed that the method of upper bound and lower bound for predicting the ultimate capacity is valid.

ACKNOWLEDGMENTS

The writer wishes to express his sincere thanks to his advisor Dr. A.M. Lansdown, M.E.I.C., M.I.A.B.S.E. Head of the Civil Engineering Department, University of Manitoba for his advice and encouragement throughout this research project.

The help of the technicians in the Civil Engineering Laboratory who assisted in the construction and testing of the model is much appreciated. A special thank is also extended to the Canadian International Development Agency for providing financial assistance during the period of study in Canada.

Finally, the writer is particularly grateful to his wife who remained at home in Thailand with two small children, for her devotion and understanding during his two-year absence.

LIST OF TABLES

<u>TABLE</u>		<u>Page</u>
1.	Dimension and Loading of Prototype and Model	10
2.	Summary of Plastic Ultimate Strengths of Beams	17
3.	Steel Properties	21
4.	Concrete Properties	22
5.	Calculation of the Ultimate Load for the Model	55

LIST OF FIGURES

<u>FIGURE</u>		<u>Page</u>
1.	Model Diagram	9
2.	Arrangement of Girders in Short Skew Crossing	12
3.	Arrangement of Girders in Wide Skew Crossing	12
4.	Arrangements of Transversal Beams	14
5.	Possible Modes of Failure	16
6.	Arrangement of Gauge Positions	25
7.	Arrangement of Supports and Loaded Points	25
8.	Relation between Gauge Pressure and Total Load	28
9.	Failure Pattern of the Model	34
10.	Sketches showing Pattern of Cracks after Testing the Model ..	36
11.	Load-Deflection Curves at Loaded Points 5, 8	39
12.	Load-Deflection Curves at Loaded Points 6, 7	40
13.	Load-Deflection Curves at Points 1, 2, 3 and 4	41

LIST OF PHOTOGRAPHS

<u>PHOTO</u>		<u>Page</u>
1.	Plywood formwork of the model	18
2.	Reinforcement details at the corners	19
3.	Reinforcement details at the joints	20
4.	Overall view of the steelwork	20
5.	Fitting of the steelwork into the formwork	21
6.	Overall view of the model after removal of the form ...	23
7.	Types of supports	24
8.	Arrangement of deflection gauges	26
9.	Overall view of the model on the testing frame	26
10.	Hydraulic loading apparatus	27
11.	Attachment of measuring scales for checking deflections	29
12.	Crushing of concrete on the top fibre at the joint	32
13.	Movement of two-directional support	33
14.	The model structure after collapse (viewed from the top)	33
15.	The model structure after collapse (viewed from the side)	35
16.	Shear cracks near the supports	35
17.	Bottom view of crack pattern; left side	37
18.	Bottom view of crack pattern; right side	37

LIST OF PHOTOGRAPHS (CONTINUED)

<u>PHOTO</u>		<u>Page</u>
19.	Bottom view of crack pattern	38
20.	Twisting of the longitudinal beam	38
21.	Cracks at the joint	43
22.	Cracks at the hinge point due to bending and torsion ..	43

NOTATION

A cage	cross section area enclosed by reinforcement
A _m	steel area in model
A _p	steel area in prototype
	$A_m = \left(\frac{l}{\lambda} \right)^2 A_p$
A _s	steel area
C	circumference of cage
f _m	stress in model
f _p	stress in prototype
	$f_m = f_p$
f' _c	compressive strength of concrete
f _y	yield stress of steel
F _{yL}	yield strength of one longitudinal bar
F _{yT}	yield force per unit length of beam
L _p	dimension of prototype
L _m	dimension of model
	$\lambda = \frac{L_p}{L_m}$
M _B (●)	positive bending strength of beam
\bar{M}_B	negative bending strength of beam
M _T (○)	torsional strength of beam
M _m	moment in model
M _p	moment in prototype (or plastic moment)
	$M_m = \left(\frac{l}{\lambda} \right)^3 M_p$
n	numbers of longitudinal bars

NOTATION (CONTINUED)

p	pitch of stirrups
P _m	concentrated load on model
P _p	concentrated load on prototype
		$P_m = \left(\frac{1}{\lambda} \right)^2 P_p$
P _u	ultimate point load
R _{min}	$\frac{nF_y L}{C}$ or $\frac{F_y T}{p}$ whatever is lesser
W _E	external workdone by the load
W _D	work dissipated in the hinges
ε _m	strain in model
ε _p	strain in prototype
λ	linear scale = $\frac{L_p}{L_m}$
δ	deflection under load
θ	rotation of beam or mechanism
α	skew angle
φ	diameter of bars

CHAPTER I

INTRODUCTION AND REVIEW

1.1 Introduction

The development of modern highways for present day traffic has required the design of skew bridges to accommodate greater speed and heavy truck loads. Reinforced and prestressed concrete slabs are of particular importance for bridges as they will accommodate heavy truck loads and are suitable for short span. However, it is uneconomical to build a full scale structure for testing and study in the laboratory. The use of small-scale models has been developed⁽¹⁾ to produce valid results under most circumstances, although some factors omitted in the design of the model may cause a difference between tested and calculated results.

The analysis of most of the previous work was based on working stress. This method of analysis neglects many important factors which if considered can result in substantial savings in bridge design. In addition many simplifying assumptions have been made in order to develop the design method. The utilization of the strength of mild steel was limited to a fraction of the proportional limit, and the reserve strength above the yield point also neglected. This is why the elastic theory is considered to be conservative in design. On the other hand, the plastic theory utilizes the reserve strength and deformation of mild steel above the point of first yielding. It is applicable to both steel and reinforced concrete structures. The calculation simply involves the work dissipated

in the hinge or mechanism being equal to the external work done, or the loss of potential energy. And the analysis involves an equilibrium check (work equation) and check on yield criterion ($M \ll M_p$). It is relatively simple, easy to understand, and particularly applicable for mild steel. For these reasons this method of calculation is widely used in developed countries.

Because of the scarcity of reports of previous work in the case of grillage bridges it was decided to confine the study to an open grillage. The treatment of open grillage bridges is similar to that which would be used for buildings designed as open frame.

1.2 Review of Elastic and Plastic Theories

In 1938, Hetenyi^(a) introduced a method of calculating grillage beams subjected to a concentrated load. Cecilia Vittoria Brigatti^(b) attempted to apply Macus's method of handling difference equation to skew slabs with uniformly distributed load during the same year. However, his fundamental equations proved to be in error later. Anzelius^(c) solved a 45-degree skew slab having a uniformly distributed load and simply supported on two opposite sides by differential equations in 1939. In 1940, Helmut Vogt^(d) also analyzed skew slabs subjected to a uniformly distributed load and simply supported at two opposite edges. Jensen^(e) determined the behaviour of skew slabs by means of difference equations in 1941. In 1947, Jensen and Allen^(f) analyzed skew slab bridges with curbs of skew angles of 30-, 45- and 60- degrees by difference equations.

They also tabulated the influence surfaces for moments at various points of concentrated loads on slabs. Newmark^(g) conducted tests of a simple-span skew I - beam bridges in 1948. His tests involved: (i) influence lines tests for strains and deflections in the beams and strains in the slab reinforcement and (ii) tests with simulated wheel loads with one and two wheel loads at various points on the slab. In 1950, Gossard^(h) performed a test on highway skew slab bridges with curbs. The skew angles were 45- and 60- degrees. The purposes of his tests were (i) to compare the actual behaviour of the bridges in both the uncracked and cracked states with the behaviour predicted by the theory of isotropic slabs, and (ii) to observe conditions at and near the ultimate loads. The results were summarized and discussed in his paper.

In 1951 and 1952 Heyman^(i,j) described a method of limit design of transversely loaded square grids by using the assumptions of plastic theory as applied to steel structures. Morice^(k) (1956) applied the yield line theory to investigate the minimum transverse strength of slab bridges. The result showed that the use of an ultimate load analysis and a consistent factor of safety may lead to very great reductions in the transverse strength required for solid slab bridges. Reynold^(l) (1957) employed the yield line method to analyze the strength of right angle prestressed concrete slab bridges with edge beams. His analysis gave results which were in good agreement with experimental results. In the same year Reynold^(m) also applied plastic theory to prestressed concrete grillage bridges both in right angle and skew bridges. The ultimate load for each model was in

excess of the predicted ultimate load, for a number of reasons, which were discussed in his paper. Chen⁽ⁿ⁾ (1957) using difference equation analyzed the moments in simply supported skew I-beam bridges and tabulated the influence coefficients for moments in beams, slabs and deflections of beams. In 1962, Rowe^(o) and Jone^(p) each discussed the ultimate strength of skew slabs in text books on concrete structures. Lansdown^(q) (1964) developed and explained the effect of plastic torsion in reinforced concrete beams and the method of combined yield lines and yield hinges for composite structures. Yih^(r) (1967) conducted a model test of reinforced concrete skew slab and beam bridges under ultimate loads at the University of Manitoba. And Somsak T.^(s) (1968) also conducted test of right angle reinforced concrete slab bridge decks under ultimate loads at the same university. The analysis in each case was based on the combination of yield-line theory and yield hinge theory.

1.3 Object of the Test:

The method of yield hinge theory was used in this study to analyze a skew grillage bridge. The model was simply supported at the two opposite sides and was loaded by four wheel loads simultaneously applied to the four middle node points (assumed critical loading). It was designed to accommodate two lanes of traffic using a reduced H20 - S16 highway loading. The model considered was one-fourth scale skew grillage bridge with a skew angle of 30 degrees.

The principal object of the test was to compare the behaviour of

the one-quarter scale model with that predicted by the yield hinge theory. In particular, the maximum load carrying capacity and deflections at failure were observed, and the load-deformation characteristics obtained.

1.4 HISTORICAL BIBIOGRAPHY

- (a) Hetenyi, M.
(1938) "A Method of Calculating Grillage Beams" S. Timochenko 60th Anniversary Volume. New York, 1938 PP. 60-72.
- (b) Cecilia Vittoria Brigatti
(1938) "Applicazione del metodo di H. Marcus al Calolo della piastra parallelogrammica" Richerche di Ingegneria, Vol. XVI, March - April 1938, No.2, P.42.
- (c) Adolf Anzelius
(1939) "Über die elastische Deformation parallelogramm forminger Platten". Der Bauingenieur, Vol. 20, Sept. 1939, No. 35/36, P.478.
- (d) Helmut Vogt
(1940) "Die Berechnug Schiefwinklier Platten und plattenartiger Brücken systeme", Beton und Eisen, 39, No.17, Sept. 1940, P.243-245.
- (e) Vernon P. Jensen
(1941) "Analysis of Skew Slabs". University of Illinois Bulletin Series No.332, Sept. 9, 1941. No.3.
- (f) Vernon P. Jensen and John W. Allen.
(1947) "Studies of Highway Skew Slab-Bridges with Curbs". University of Illinois Bulletin Series No.369, Sept. 19, 1947. No.8.
- (g) Nathan M.Newmark, Chester P. Siess and Warren M. Peckham
(1948) "Studies of Slab and Beam Highway Bridges". Part II. "Tests of simple-span skew I-beam bridges". University of Illinois Bulletin Series No.375, Jan. 12, 1948, No. 31.
- (h) Myron L. Gossard
(1950) "Studies of Highway Skew Slab Bridges with Curbs" Part II. Laboratory Research. University of Illinois Bulletin Series No. 386, Feb. 1950, No.46.
- (i) Heyman, J.
(1951) "The limit design of space frames". Journal of Applied Mechanics. Vol. 18, No.2, June 1951.
- (j) Heyman, J.
(1952) "The limit design of transversely loaded square grid". Journal of Applied Mechanics Vol. 19. No. 2, June 1952.

- (k) Morice, P. B.
(1956) "The minimum transverse strength of slab bridges". Magazine of Concrete Research, Cement and Concrete Association, Vol. 8 No. 23, Aug. 1956.
- (l) Reynold, G. C.
(1957) "The Strength of right prestressed concrete slab bridges with edge beams". Magazine of Concrete Research, Cement and Concrete Association. Vol. 9, No. 27, Nov. 1957.
- (m) Reynold, G.C.
(1957) "The strength of prestressed concrete grillage bridges". Technical Report, Cement and Concrete Association. June 1957, TRA/268.
- (n) Chen, T. Y., C.P. Siess and N. M. Newmark
(1957) "Moments in Simply Supported Skew I-beam Bridges". Studies of slab and beam highway bridges. Part VI, University of Illinois Bulletin Series No. 439, Vol. 54 Jan. 1957.
- (o) Rowe, R. C.
(1962) "Concrete Bridge Design". John Wiley & Sons, Inc. Newyork 1962.
- (p) Jones, L. L.
(1962) "Ultimate load analysis of reinforced and prestressed concrete structures". Chatto & Windus Ltd. London 1962.
- (q) Lansdown, A. M.
(1964) "An Investigation into the Ultimate Behaviour of Reinforced Concrete Beam and Slab Structures, in Particular Bridge Decks". Ph.D. Thesis, University of Southampton, June 1964.
- (r) Jenn-Ching Yih
(1967) "Model Studies of Reinforced Concrete Skew Slab and Beams Bridges under Ultimate Load". M. Sc. Thesis, University of Manitoba.
- (s) Somsak T.
(1968) "A Study of Reinforced Concrete Beam and Slab Bridge Decks under Ultimate Load". M. Sc. Thesis, University of Manitoba.

CHAPTER II

DESIGN OF A SKEW GRILLAGE BRIDGE

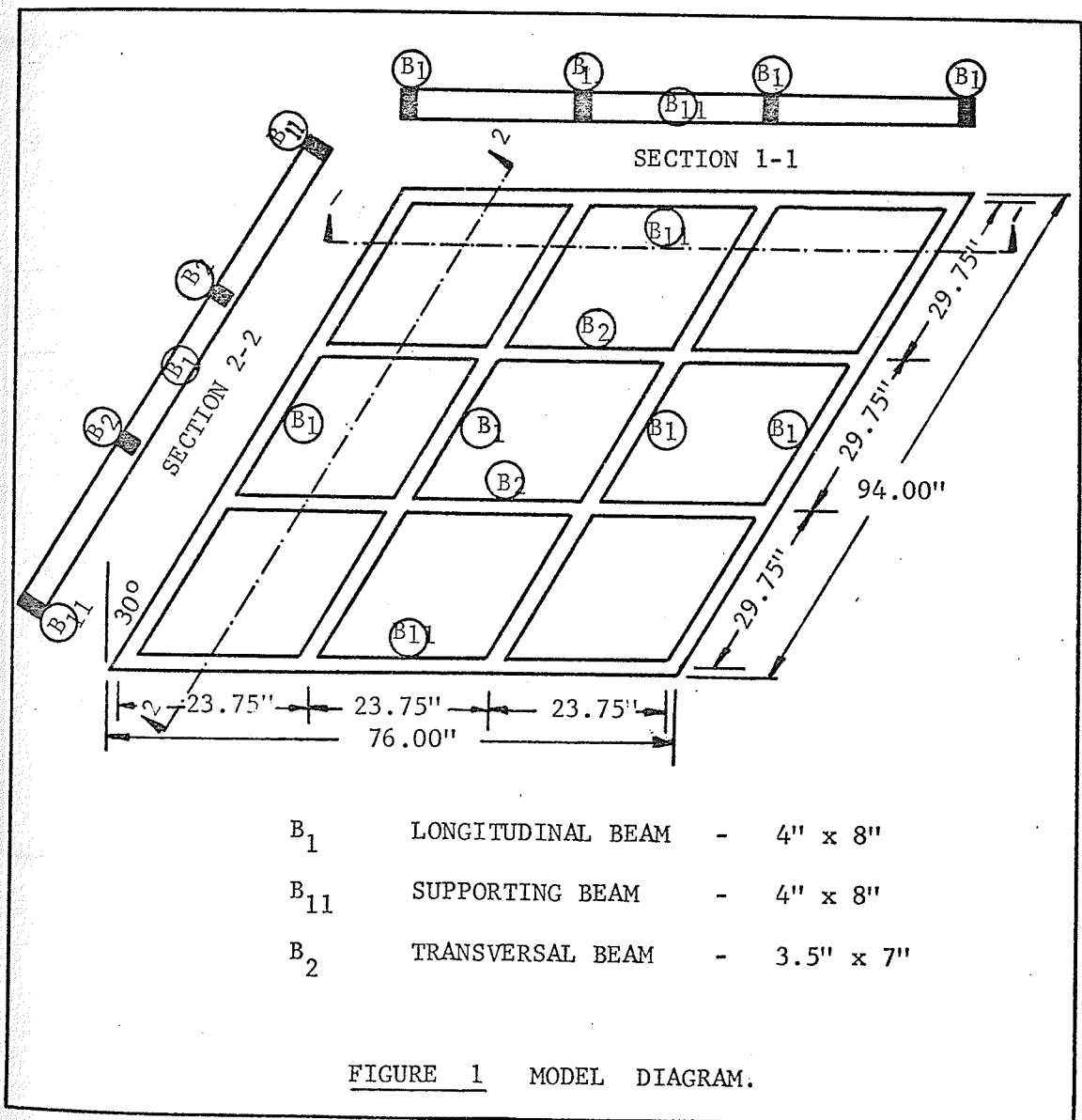
2.1 General Considerations

A prototype considered here was a simply supported skew grillage bridge having a skew angle of 30 degrees. It was designed to accommodate two lanes of traffic with H20 - S16 truck loading. The prototype had a span length and roadway width of 30 feet and 24 feet respectively. The structure was designed to carry the maximum bending moment for the specific points of the wheel loads on the main beams. There are many positions within the lane that the wheel loads can be applied. In general very nearly the maximum bending moment is produced when the two rear axle loads are applied symmetrically about the middle of the span length^(2,3). In this study it was assumed that two vehicles passed at the middle of the span length and the two rear axle loads for each vehicle were applied at the node points. This is not quite true in practice but in the case of grillage beams it is impossible to apply the wheel loads at other points than the node points or points along the main beams.

2.2 Description of the Skew Grillage Bridge

The 30-degree skew grillage bridge structure chosen in this study had a span length of 30 feet in the direction of the roadway and had a road width of 24 feet. It was designed for the two lane highway traffic and was composed of four main longitudinal beams placed in the direction of the roadway with a spacing of 8 feet centre-to-centre.

All longitudinal beams were of equal size, 16 inches wide by 32 inches deep and were enclosed by two supporting beams (end transversals) of the same size. Another two transversal beams 14 inches wide by 28 inches deep were located at the third points, at 10 feet centre-to-centre. The model was constructed to one-fourth of the prototype dimensions. For a detailed description, see the model diagram in Figure 1.



2.3 Scale Relations

It is uneconomical and unnecessary to build a prototype for testing, in many cases. A scale model is generally used in the laboratory for greater convenience. For this study it was considered that a one-quarter scale model would yield valid results which could be applied to the prototype. The dimensions of the prototype and the model are shown in Table 1. The other well-known scale relationships between the prototype and the model are shown in the section on Notation on Page x.

TABLE 1.

Dimensions and Loading of Prototype and Model

Description	Prototype	Model
Span length	30' - 0"	7' - 6"
Roadway width	24' - 0"	6' - 0"
Longitudinal beam spacing	8' - 0"	2' - 0"
Transversal beam spacing	10' - 0"	2' - 6"
Beams Sections		
B_1	16" x 32"	4" x 8"
B_{11}	16" x 32"	4" x 8"
B_2	14" x 28"	3.5" x 7"
Truck Load	24 kips.	1.5 kips.

2.4 Design of the Model

In general there are two ways of arranging the main girders in the case of a skew crossing:

- (i) The main girders can be placed parallel to the direction of the roadway and not at right angles to the abutments.⁽²⁾ The design span of the girders is then measured along the same direction. This method is economical for short span bridges.
- (ii) For wide skew crossings it is preferable to place the girders at right angles to the abutments. This results in triangular section at each side of the crossing and thus one end of the girder rests on the abutment and the other end on the parapet girder. The parapet girders carry heavy loads, and to increase their depth it is often desirable to extend them above the roadway. These two types of skew crossings are shown in Figure 2 and Figure 3 respectively.

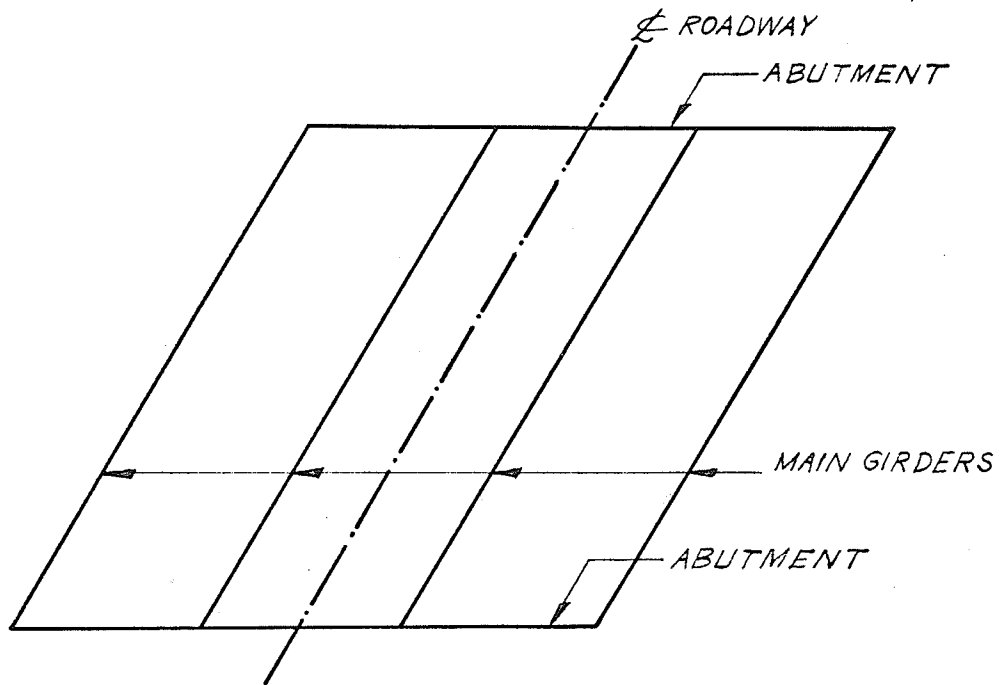


FIGURE. 2 ARRANGEMENT OF GIRDERS IN SHORT
SKEW CROSSING.

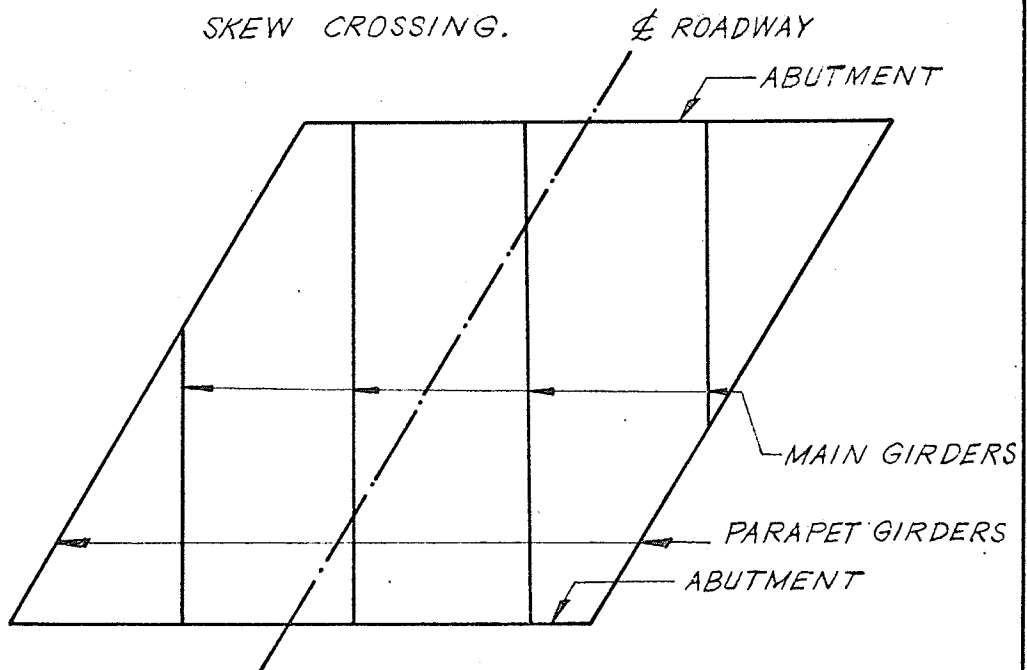


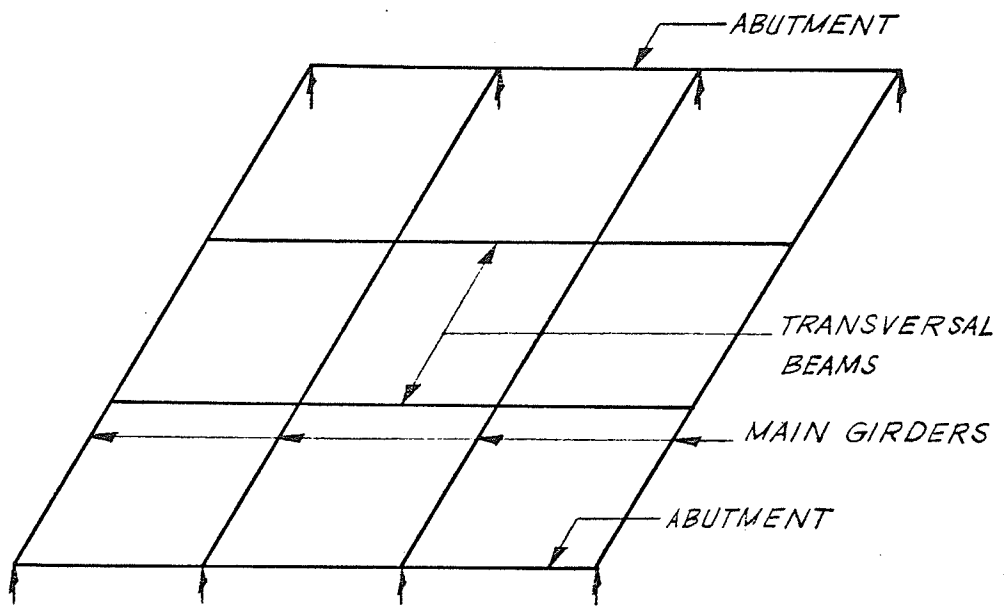
FIGURE. 3 ARRANGEMENT OF GIRDERS IN WIDE
SKEW CROSSING.

The transversal beams or diaphragms may be placed parallel to the abutments or perpendicular to the longitudinal beams. Reynolds's experiments^(4,5) revealed that there was no apparent difference in the behaviour of skew bridges with the transverse beams at right angles to the main beams and the right-angle bridges, although it would appear to be more effective to have transverse beams at right angles to the main beams than to have them parallel to the abutments (Figure 4).

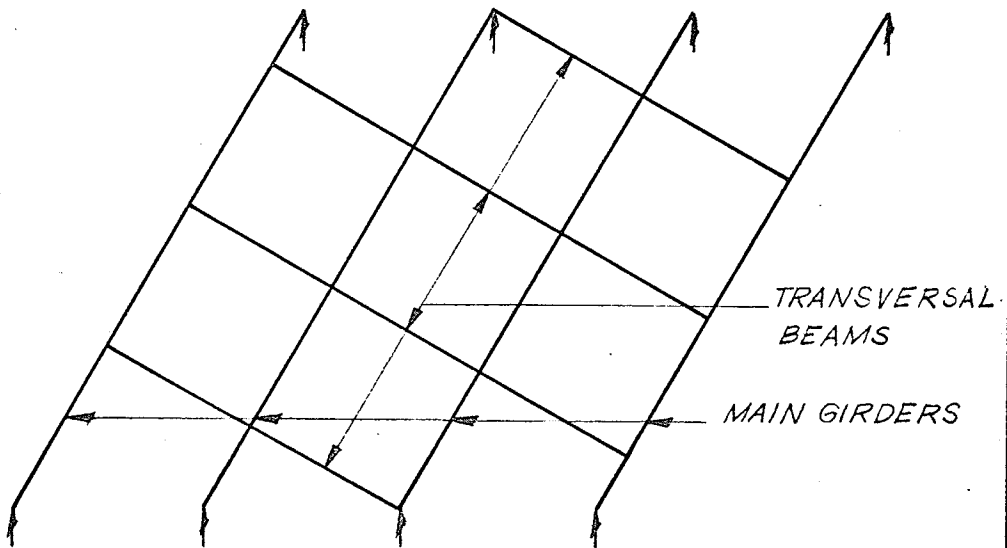
The span length of 30 feet was considered to be a short span, therefore case (i) for skew crossings was chosen for this study. The model was designed using the elastic theory according to AASHO specifications⁽⁶⁾ and by using the reduced load from the scale relations indicated in Table 1. The following assumptions were made:

- (i) The girders were simply supported and subjected to pure bending only;
- (ii) No torsional strength existed in the girders;
- (iii) The abutments caused no effect on the bending moments of the girders;
- (iv) The diaphragms or transversal beams caused no effect on the bending moments of the girders.

For simplicity of making the formwork the two outer girders were made equal to the inner girders although they carried less load.



A). TRANSVERSAL BEAMS PLACED
PARALLEL TO THE ABUTMENTS.



B). TRANSVERSAL BEAMS PLACED
PERPENDICULAR TO MAIN GIRDERS.

FIGURE. 4 ARRANGEMENTS OF TRANSVERSAL BEAMS

2.5 Determination of the Ultimate Load for the Model

The plastic theory and the method of upper and lower bounds were applied to analyze the model.⁽⁴⁾ The ultimate load for the structure was obtained by equating the workdone by the load, during collapse, to the work dissipated in the hinges. ie:

$$\sum (P \cdot \delta) = \sum (M \cdot \theta) = \sum (M_B \cdot \theta_B + M_T \cdot \theta_T)$$

The load P will be the true collapse load only if the assumed mode of failure is the correct one. The load obtained by the virtual work equation is always greater than or equal to the true collapse load. In order to obtain the lower bound for the collapse load, the structure was then examined statically under the load P. Four modes of failure were postulated for the model structure. The lowest P_u was found to be 11.20 kips, which was found to be associated with a statically admissible system.⁽⁴⁾ The ultimate load for each mechanism is shown in Figure 5, and the calculations are shown in Appendix B (Page 55). The analysis for the plastic bending moments of the beams were based on Ferguson's method⁽⁷⁾ and torsional moments based on Lansdown's.⁽⁸⁾ The detailed calculations of the bending and torsional moments are shown in Appendix A (Page 48) and summarized in Table 2.

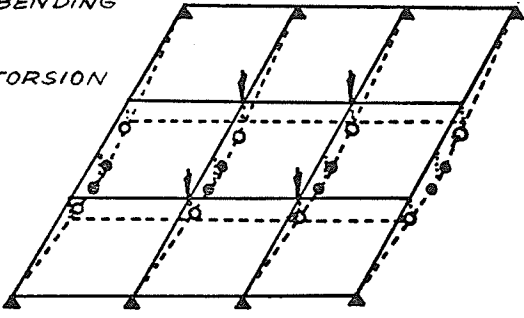
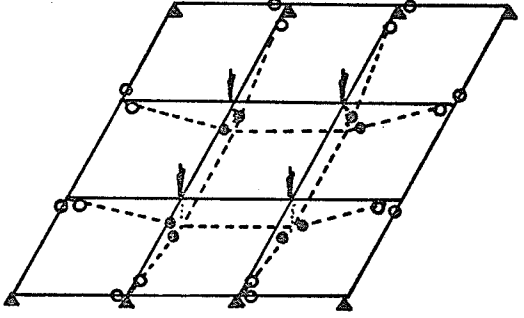
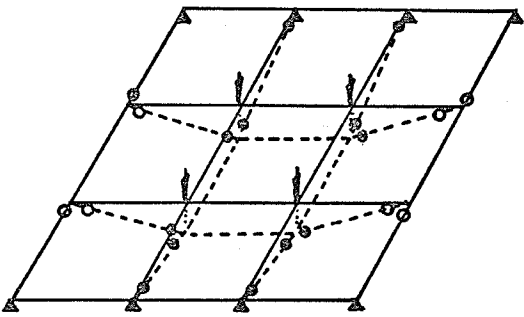
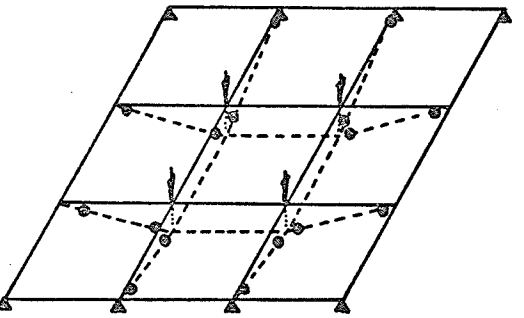
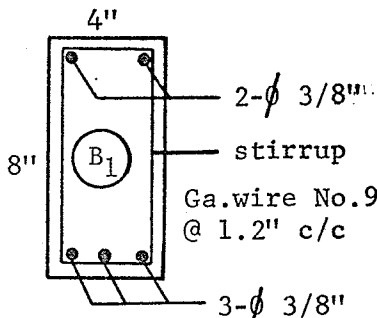
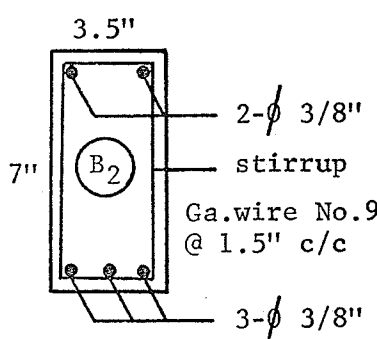
No	MODE OF FAILURE	P_U -(KIPS)
1	<p>  BENDING TORSION </p> 	11.20
2		13.64
3		15.69
4		17.86

FIGURE. 5 POSSIBLE MODES OF FAILURE

TABLE 2

Summary of plastic ultimate strengths of beams

Beam Section	M_u (in. - kips)	M_u' (in. - kips)	$M_{T,T}$ (in. - kips)
 <p>4" 8" B₁ 2-ϕ 3/8" stirrup Ga. wire No. 9 @ 1.2" c/c 3-ϕ 3/8"</p>	152.65	103.80	24.70
 <p>3.5" 7" B₂ 2-ϕ 3/8" stirrup Ga. wire No. 9 @ 1.5" c/c 3-ϕ 3/8"</p>	131.20	88.50	14.30

CHAPTER III

SPECIMEN AND TESTING APPARATUS

3.1 Model Construction

Two sheets of 3/4" thick plywood were laid flat on the laboratory floor. The side forms of 3/4" plywood were fastened to the bottom to form the sides. The bottom and sides were fastened with screw nails and the side forms were rigidly anchored by the triangular pieces of wood as shown in Photo 1. The inside surface of the formwork was shellacked and oiled after construction. The 3/8-inch reinforcing steel was cut to length and bent accordingly to ACI Standards for Bending Bars.⁽⁹⁾ The stirrups of No. 9 gauge wire were bent carefully to the sizes of the cages of the beams by using a jig.

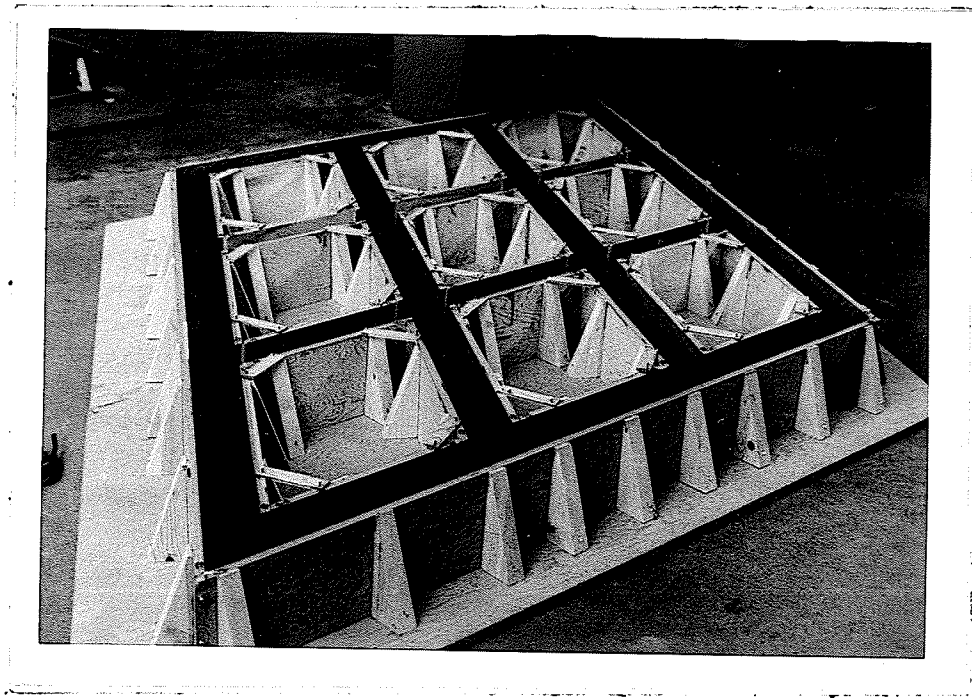


Photo 1. Plywood formwork of the model

The main reinforcement and stirrups were tied together using standard ties. At the four corner joints the main reinforcement was bent to overlap and two pieces of 3/8-inch bar were inserted to avoid corner failure. This is shown in Photo 2. At the joint between the longitudinal beams and the central transversal beams, two pieces of 3/8-inch bar were inserted as an anchorage to avoid the joint failure as shown in Photo 3. Four lifting hooks were placed at the corners as shown in Photo 4. The reinforcing for each beam was built separately and then all formed together to a shape of the model as shown in Photo 4. The steelwork was then put into the formwork as shown in Photo 5.

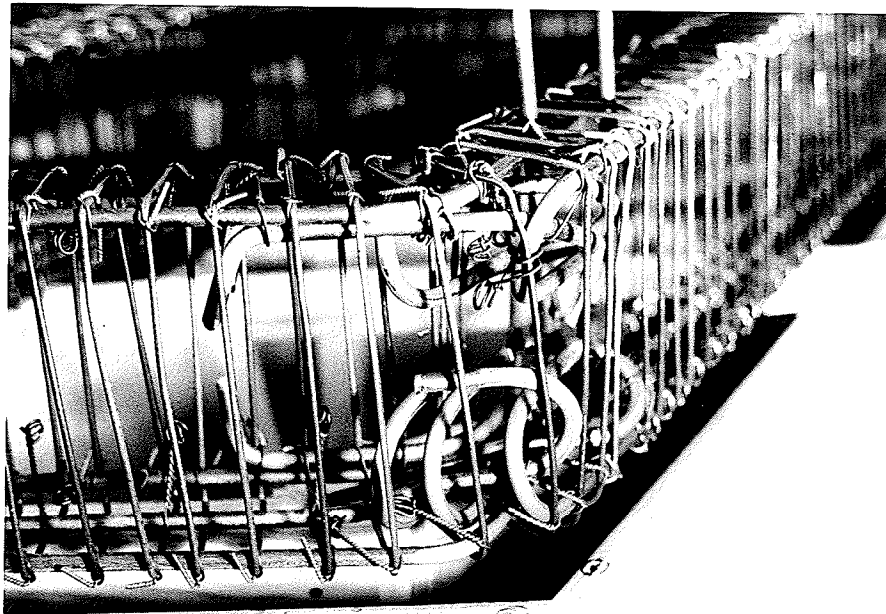


Photo 2. Reinforcement details at the corners.

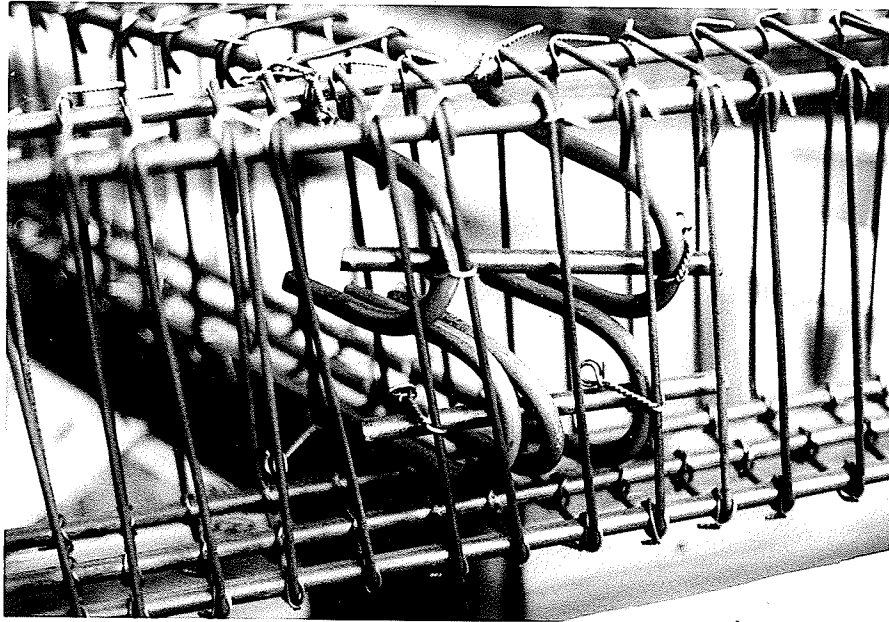


Photo 3. Reinforcement details at the longitudinal and transversal joints.



Photo 4. Overall view of the steelwork.

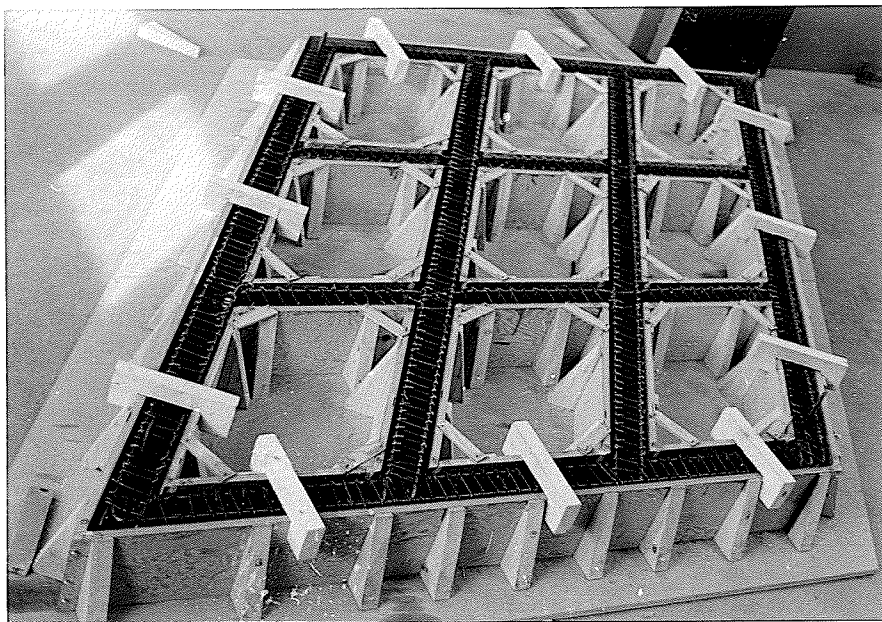


Photo 5. Fitting of the steelwork into the formwork.

3.2 Material Properties

Reinforcing steel used was of an intermediate grade, round bars of average yielding point 66 ksi. The stirrups were a mild steel of average yielding point 33 ksi. Steel properties are shown in Table 3.

TABLE 3

Steel Properties

Bar	Mean Diam. (in.)	Area (in. ²)	Av. Yield Load (lb.)	Av. Yield Strength (psi.)
9 Ga.	0.144	0.0163	538	33,000
3/8" ϕ	0.375	0.1104	7260	66,000

The concrete placed in the form was mixed by a standard concrete mixer in the laboratory following the mixing procedure defined by the section, "Laboratory Concrete Mixing".⁽¹⁰⁾ High early strength concrete and aggregate having a maximum size of 3/8-inch was used, and the concrete had a water-cement ratio of 0.62. Four 3-inch by 6-inch test cylinders were retained from each batch of concrete. The strength determined from the 3-inch by 6-inch cylinders was reduced by 6% to make valid comparison with tests from standard sized test cylinders.⁽¹⁰⁾ Concrete properties are listed in Table 4.

TABLE 4

Concrete Properties

Age (Days)	3" x 6" Cylinder Av. Crushing Load (lb.)	Av. Adjusted Compression Strength - f'_c (psi.)
7	33,700	4474
42 (Testing day)	45,600	6062

One day after the concrete was poured the forms were removed from the sides, Photo 6. The entire model was then covered with burlap and kept wet for 3 days and then placed into position on the testing frame. The model was supported by eight supports, four points under each of the supporting beam. Three types of support were used, they were fixed direction, one direction free, and two directions free, as shown separately in Photo 7. Eight dial gauges for deflection readings were attached at the bottom of the model by means of steel angles and magnetic bases. The positions of gauges and support arrangements are shown in Figure 6 and Figure 7 respectively. The attachment of deflection gauges are also shown

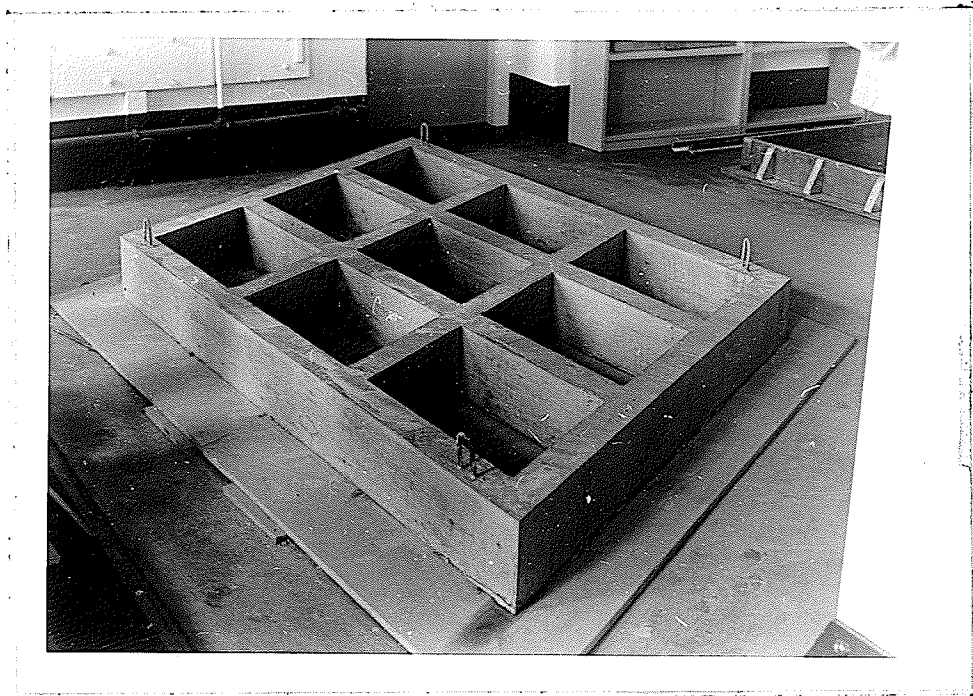


Photo 6. Overall view of the model after removal of the forms.

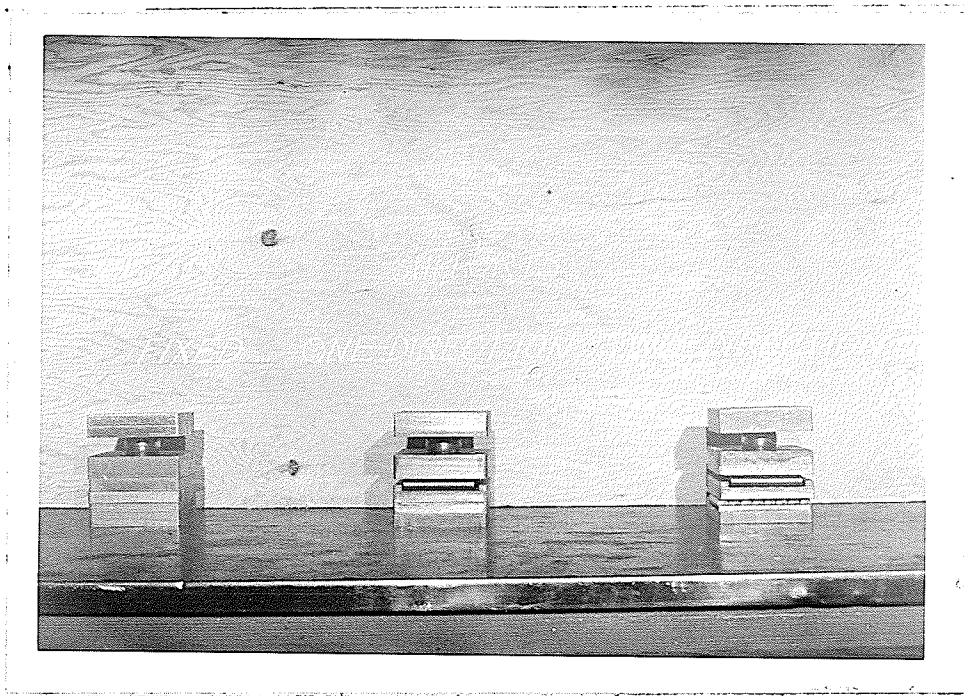


Photo 7. Types of supports

in Photo 8. Four steel angles were clamped at the outer faces of the supporting beams by means of C - clamps to prevent sliding of the model during testing. The overall view after set up of the model on the testing frame is shown in Photo 9.

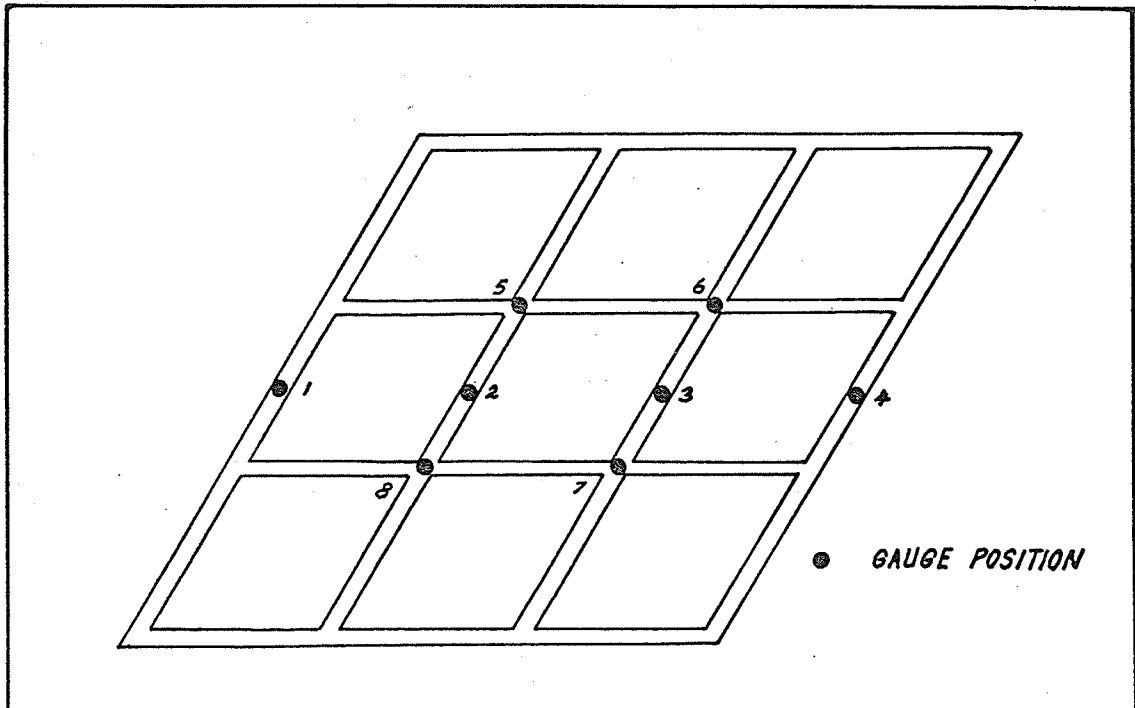


FIGURE . 6 ARRANGEMENT OF GAUGE POSITIONS.

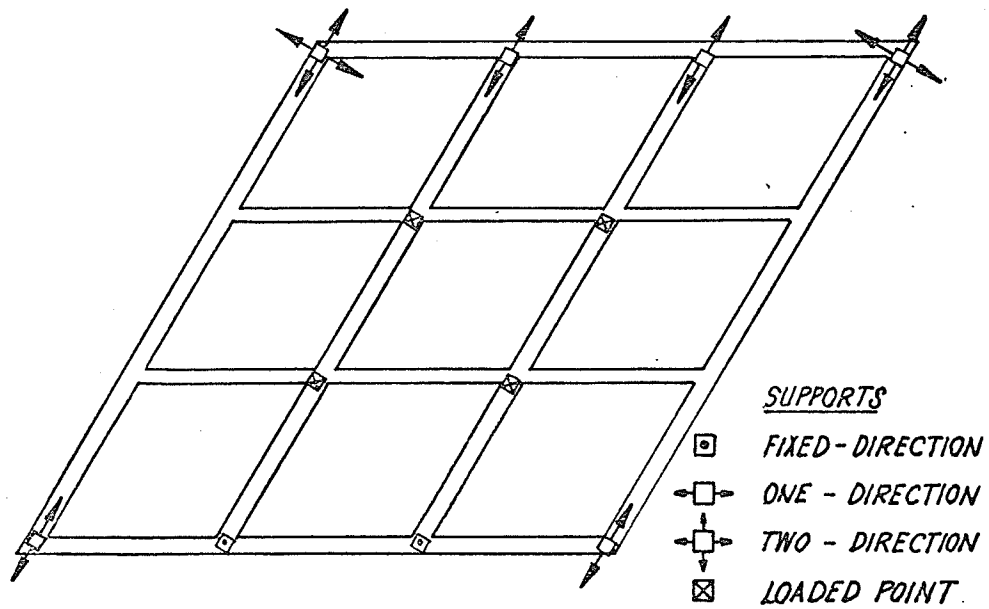


FIGURE . 7 ARRANGEMENT OF SUPPORTS & LOADED POINTS.

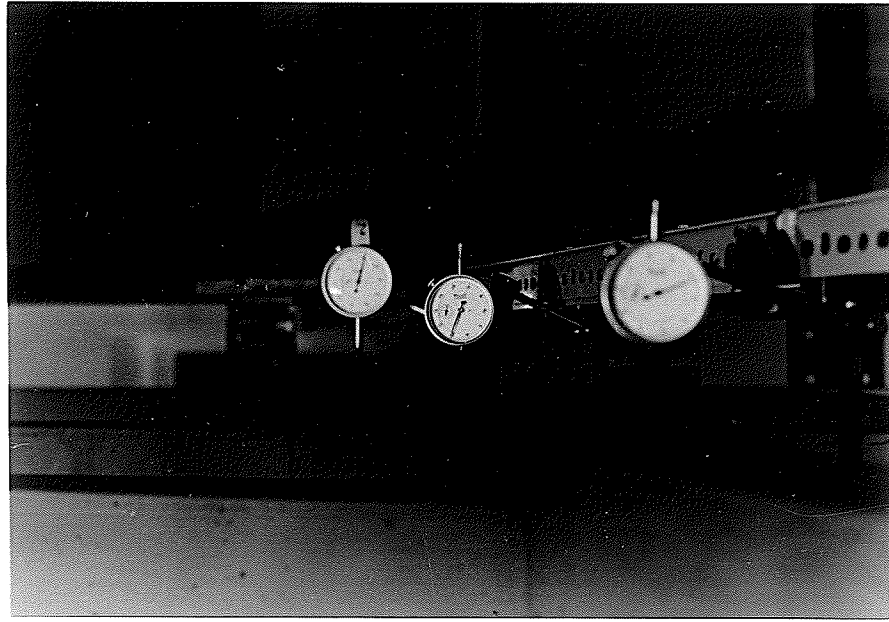


Photo 8. Arrangement of deflection gauges.

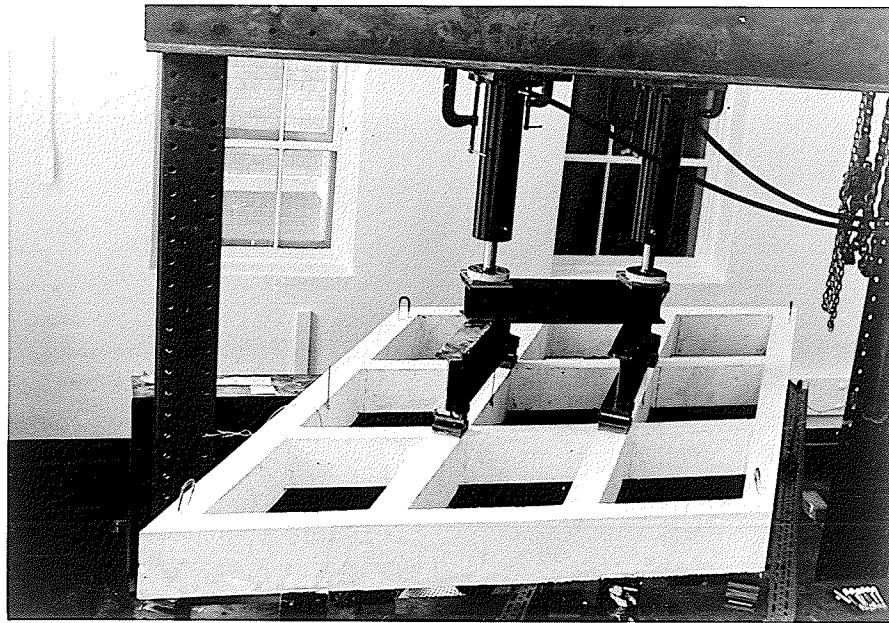


Photo 9. Overall view of the model on the testing frame.

3.3 Testing Apparatus

The testing frame resembled a portal frame. It consisted of two vertical steel columns connected by two channels on the top. The bottom of the columns were connected to the base which consisted of two steel Wide Flange beams. Two 36-inch beams were laid over the base as the supports for the model. The loading apparatus consisted of a hand hydraulic pump and two hydraulic jacks. The pump had a capacity of 2000 psi., and the jacks each had a capacity of 30,000 lb. The hydraulic pump was connected to the jacks and was calibrated before use. The hydraulic pump is shown in Photo 10. and the relation between load and pressure for the hydraulic jacks is shown in Figure 8.

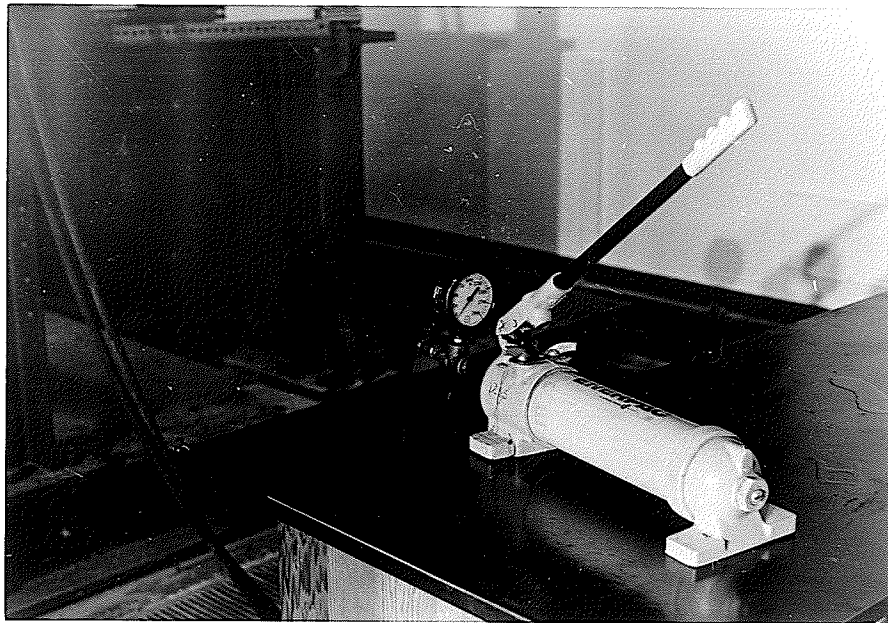


Photo 10. Hydraulic loading apparatus.

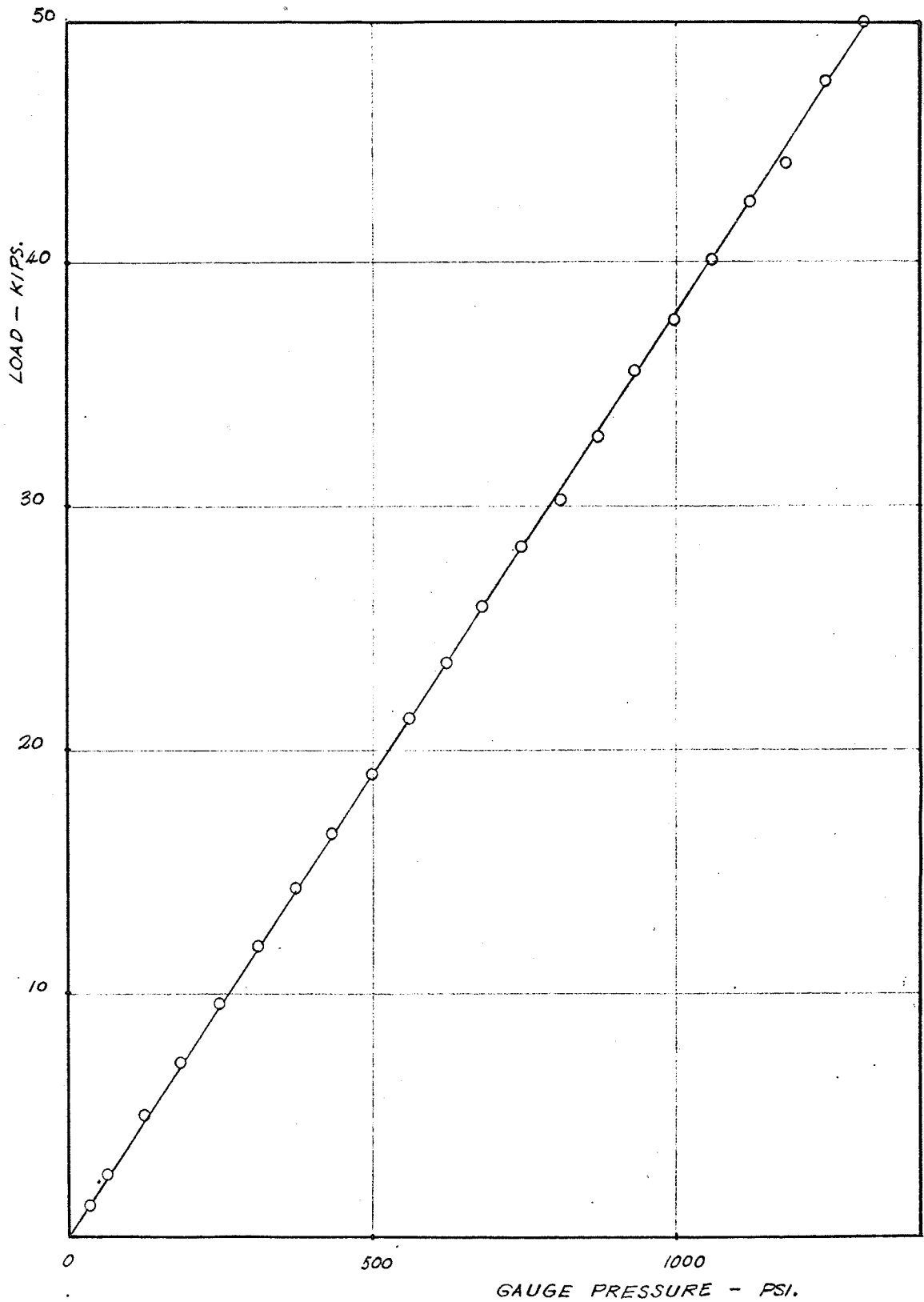


FIGURE. 8 RELATION BETWEEN GAUGE PRESSURE & TOTAL LOAD.

CHAPTER IV

TEST OF THE MODEL AND RESULTS

4.1 Testing Procedure

In this test it was assumed for the critical condition that the maximum wheel loads were applied simultaneously at the four middle node points. The load was transmitted from the two jacks to the loaded points by means of three I-beams as shown in Photo 9. (Page 26). The deflection gauges had a range of 1 inch with graduation every 0.001 in. Steel measuring scales used in conjunction with the gauges were attached to the longitudinal beams for checking the deflection and measuring the large deflections after the yielding of the steel (see Photo 11). A leveling transit was used to determine the deflections on the measuring scales. The increment of the load for each point was 300 lbs. Deflection gauge readings were taken with each increment of the load. The structure was loaded to failure with the mode of failure agreeing with the predicted mode. The deflection gauges were removed after yielding of the reinforcement.



Photo 11. Attachment of measuring scales for checking deflections.

The plastic load observed in this test was 11.10 kips. This load was maintained on the structure for 12 hours. After the end of this period it was found that the model could resist a load of 12.0 kips. The maximum deflections were measured at the points 1, 2, 3 and 4 (see Figure 6. on Page 25). Further deflection could not be obtained because of excessive rolling of the supports (see Photo 13).

It seems to the writer that the load obtained from the hydraulic jack applied directly to the structure might be slightly inaccurate. This was due to the fact that the smallest graduation on the hydraulic pressure gauge was 62.5 psi. An improved method of obtaining a precise load at each increment would be to apply the load through proving rings. In this test the load was transmitted by two hydraulic jacks through two I-beams. Care should be taken in centering the jacks on the I-beams otherwise a difference in loads might occur. The arrangement of supports also need more thought because the excessive rolling of the supports might limit the deflection readings.

4.2 Results of the Test.

The test of the model was conducted by the writer and the results are summarized as follow:

- (1) Hair cracks were first observed at a load of 3.6 kips, at the middle of inner longitudinal beams;
- (2) Yielding of the main reinforcements occurred at the load of 11.10 kips. The load of 11.10 kips. is surprisingly close to the predicted load of 11.20 kips. When those figures are compared they yield a ratio of $\frac{11.10}{11.20} = 0.99$;

- (3) After maintaining the load at 11.10 kips. for 12 hours the writer increased the load to 12 kips. and this load remained constant with increased deflection;
- (4) Increasing the load increased the deflection and finally the concrete was crushed at the top of the joint as shown in Photo 12;
- (5) The maximum deflections of the longitudinal beams at the points 1, 2, 3 and 4 were 2.63, 3.10, 2.95 and 2.70 inches respectively.
- (6) Finally the structure collapsed right across the middle of the longitudinal beams which was the mode predicted by theory, as shown in the sketch in Figure 9 and the overall view after the collapse in Photos 14 and 15;
- (7) Shear cracks developed along the longitudinal beams, see Photo 16;
- (8) Few cracks occurred along the supporting beams and transversal beams;
- (9) At the hinge points it was evident that torsional moments developed as well as the bending moments. This can be seen from the oppositely directed cracking patterns on the two faces of the longitudinal beams (see sketch in Figure 10 and Photo 17, 18). The bottom view of cracking pattern is shown in Photo 19;
- (10) Twisting of the longitudinal beams can be readily seen in Photo 20;
- (11) No evidence of failure was observed at the joints;

- (12) The support arrangements worked quite satisfactory, as the support rolled in the longitudinal direction with a slight side sway (Photo 13);
- (13) The load-deflection curves for various points were then plotted as shown in Figures 11, 12 and 13. (Readings are tabulated in Appendix C, page 60).

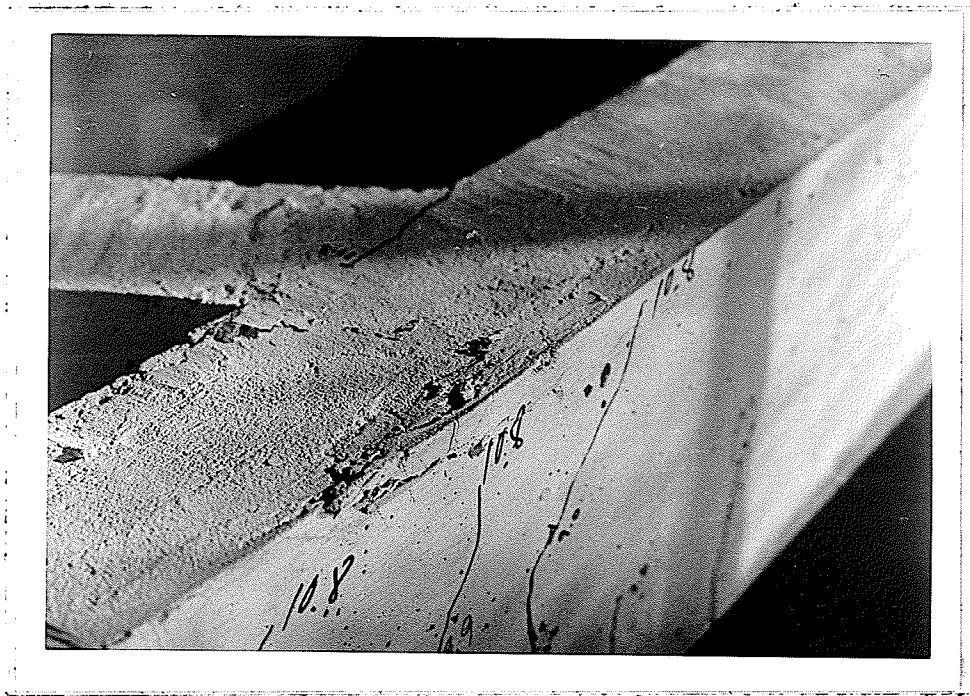


Photo 12. Crushing of concrete on the top fibre at the joint.

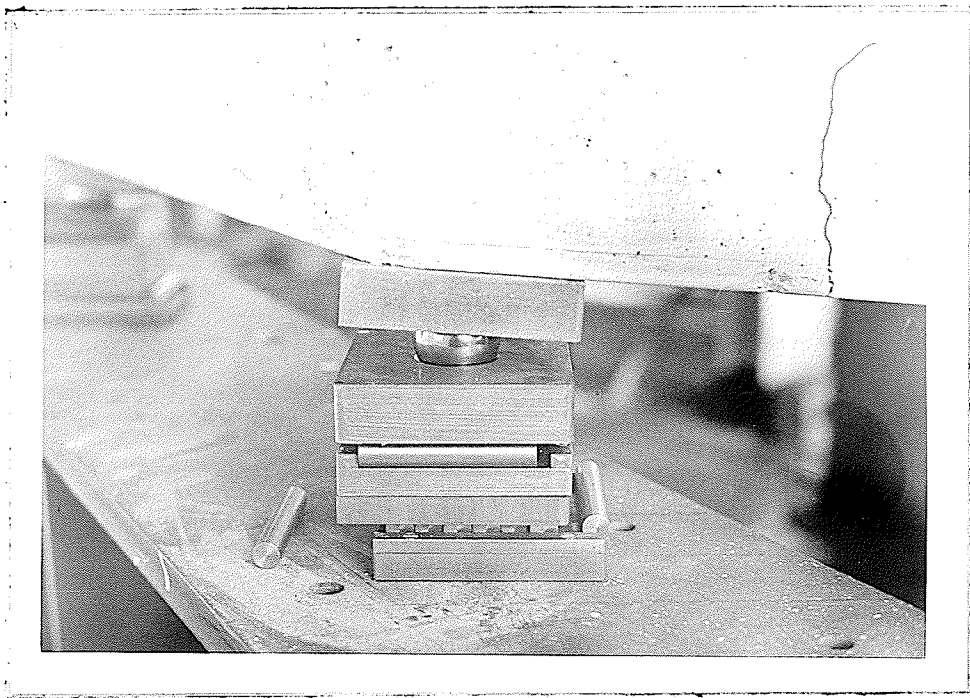


Photo 13. Movement of two-directional support.

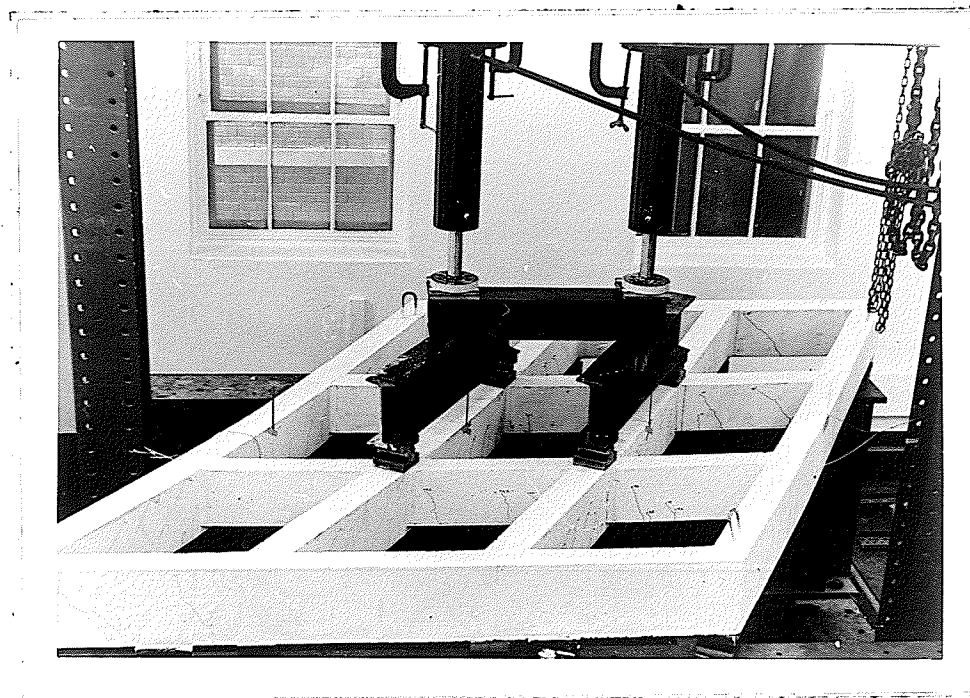


Photo 14. The model structure after collapse.
(viewed from the top)

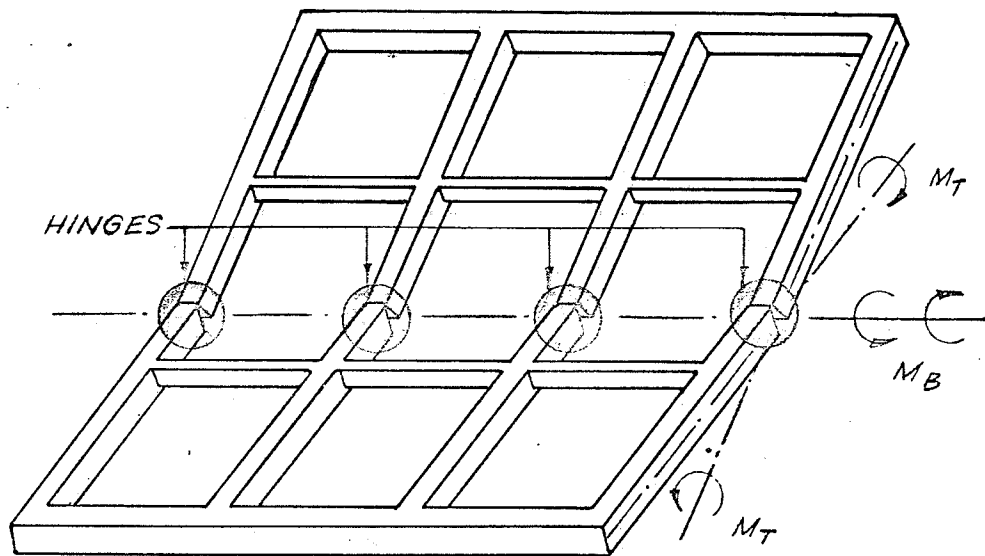


FIGURE. 9 FAILURE PATTERN OF THE MODEL

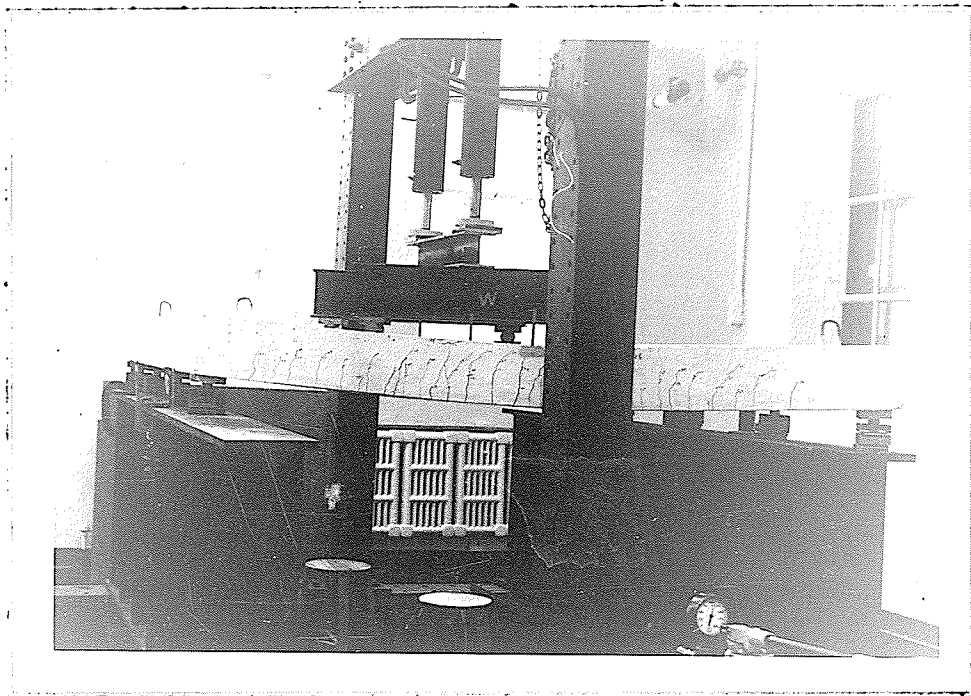


Photo 15. The model structure after collapse.
(viewed from the side)

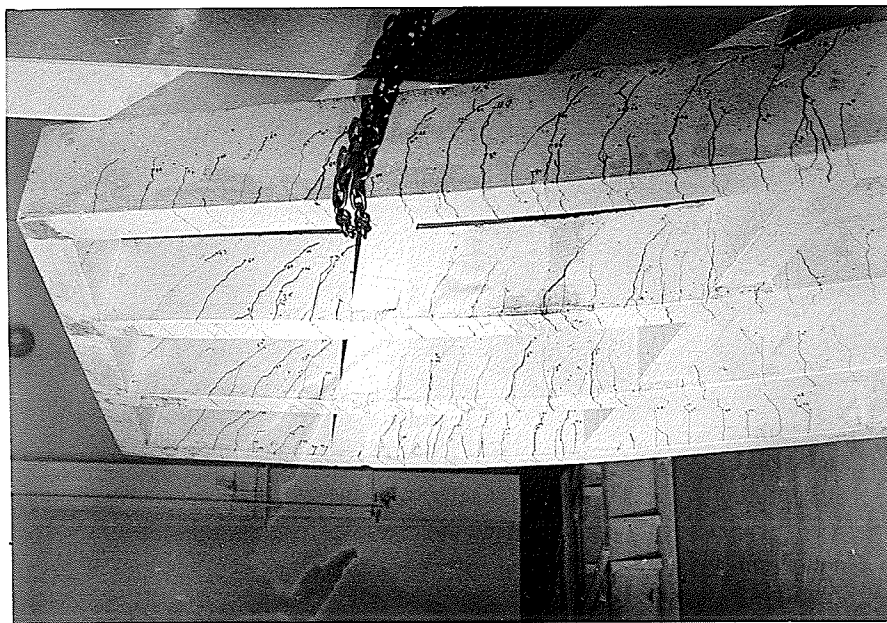


Photo 16. Shear cracks near the supports.

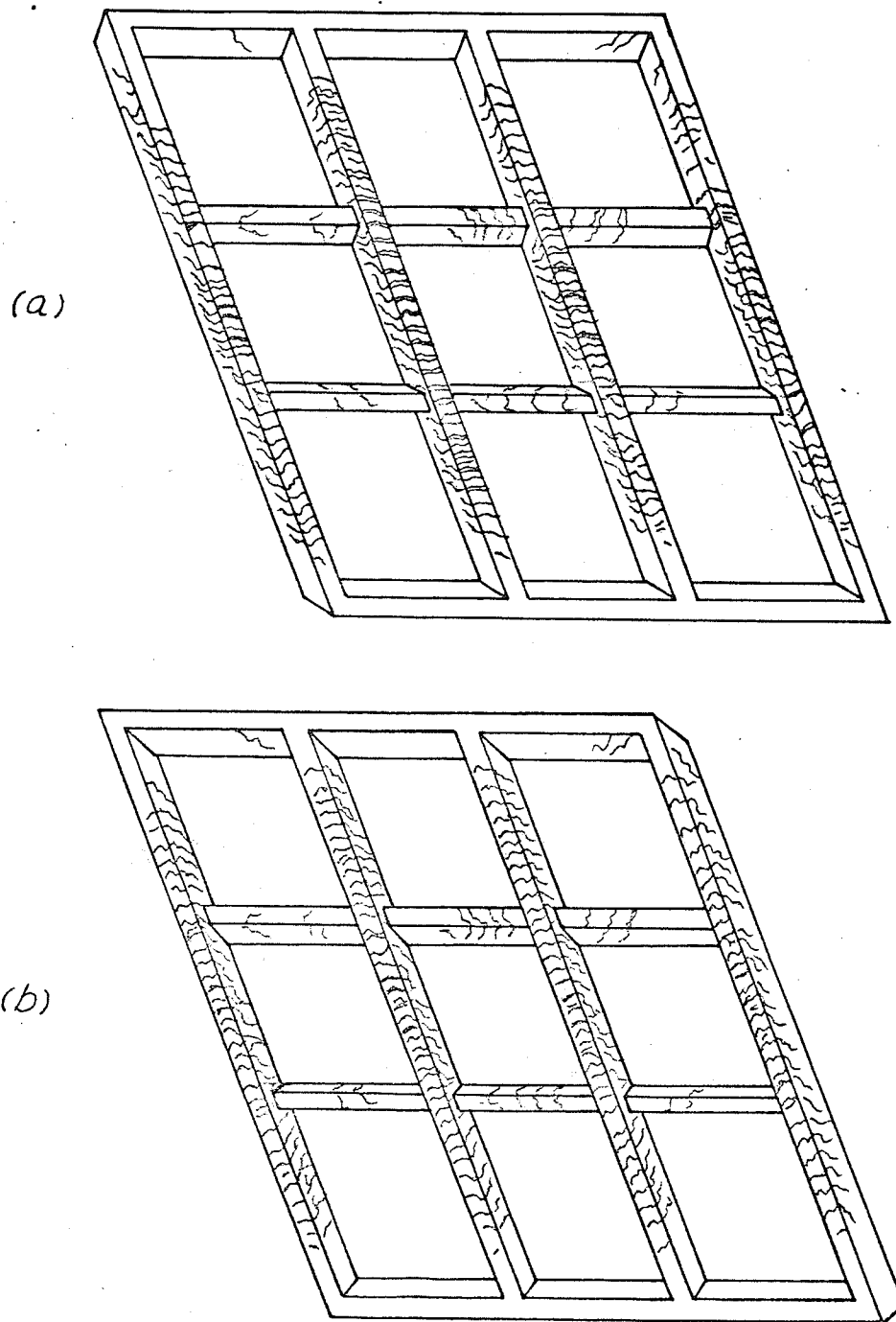


FIGURE 10 SKETCHES SHOWING PATTERN
OF CRACKS AFTER TEST IN THE BOTTOM
OF THE MODEL (a) LEFT VIEW (b) RIGHT VIEW.

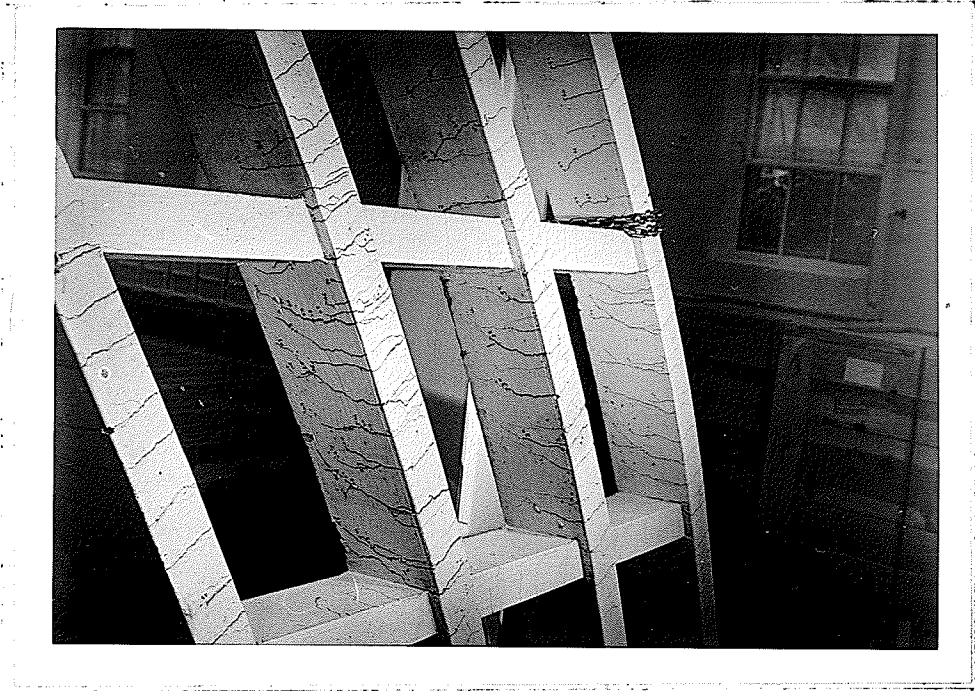


Photo 17. Bottom view of crack pattern; left side.

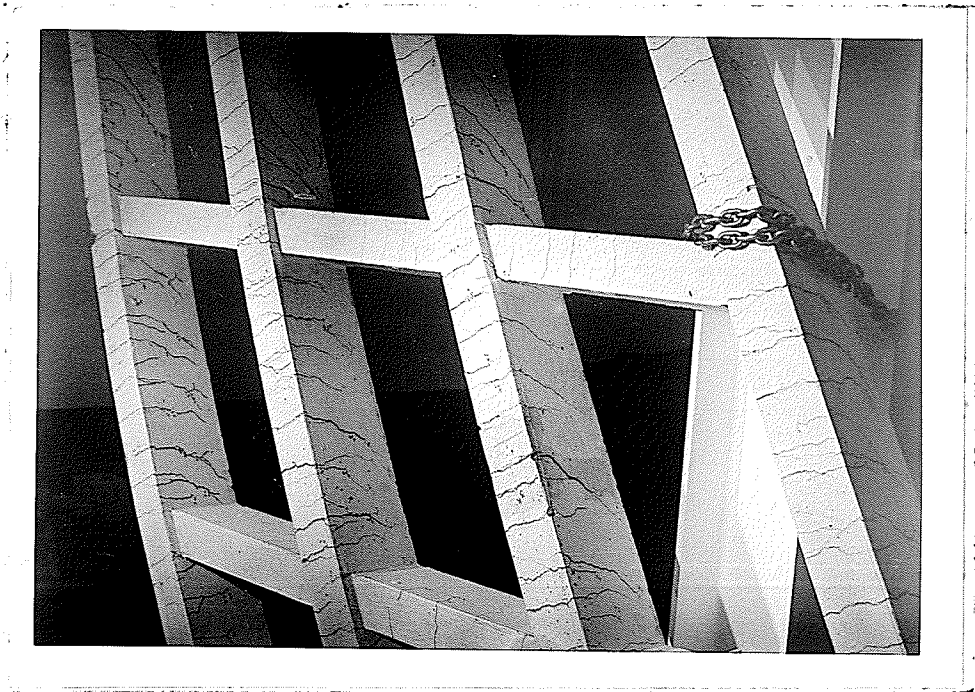


Photo 18. Bottom view of crack pattern; right side.

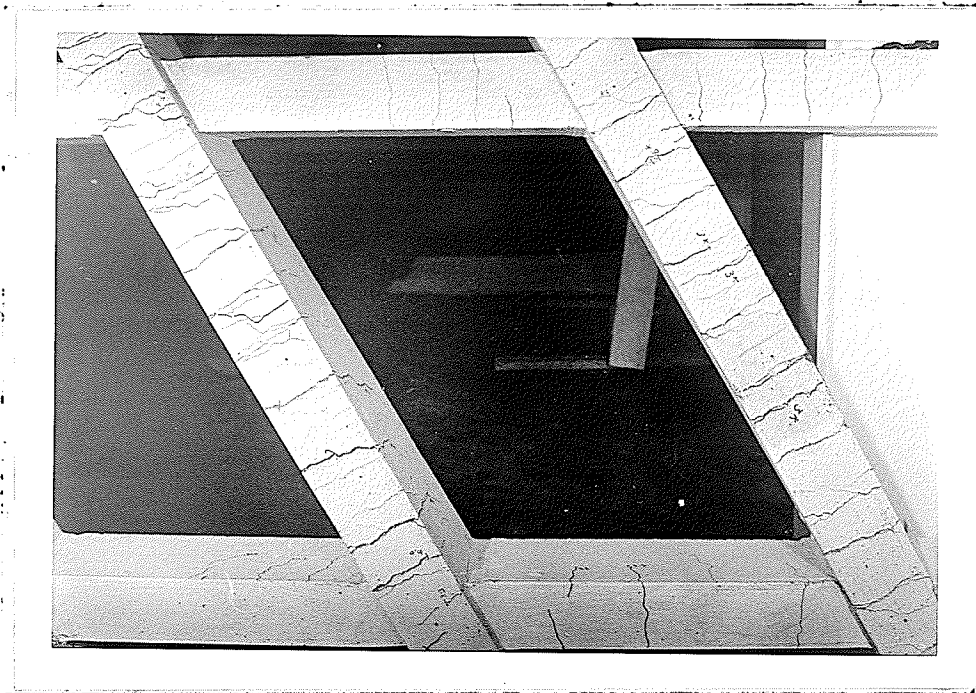


Photo 19. Bottom view of crack pattern.

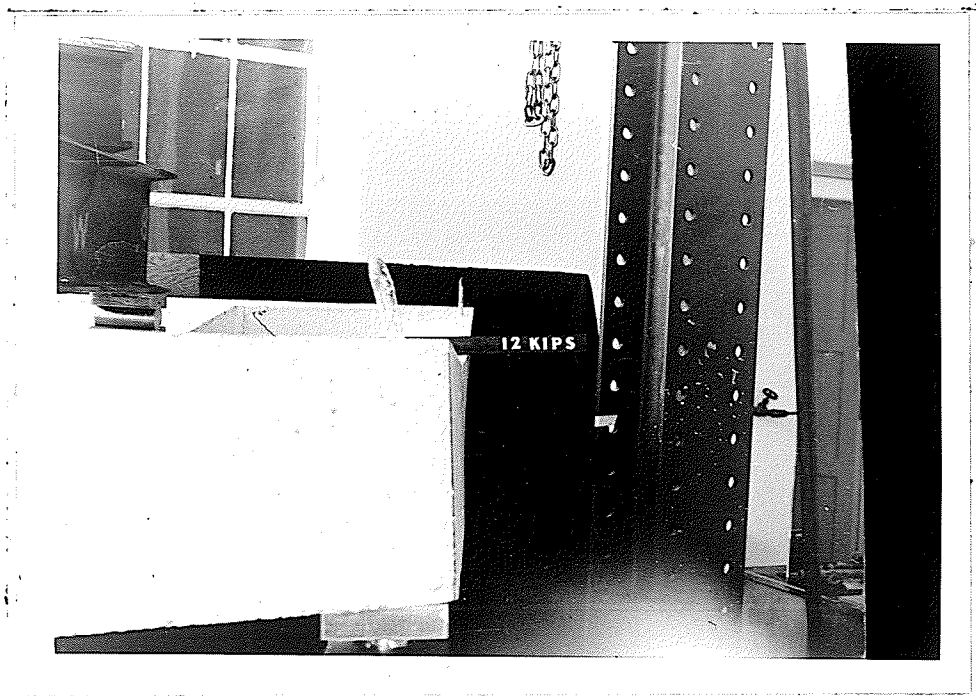


Photo 20. Twisting of the longitudinal beam.

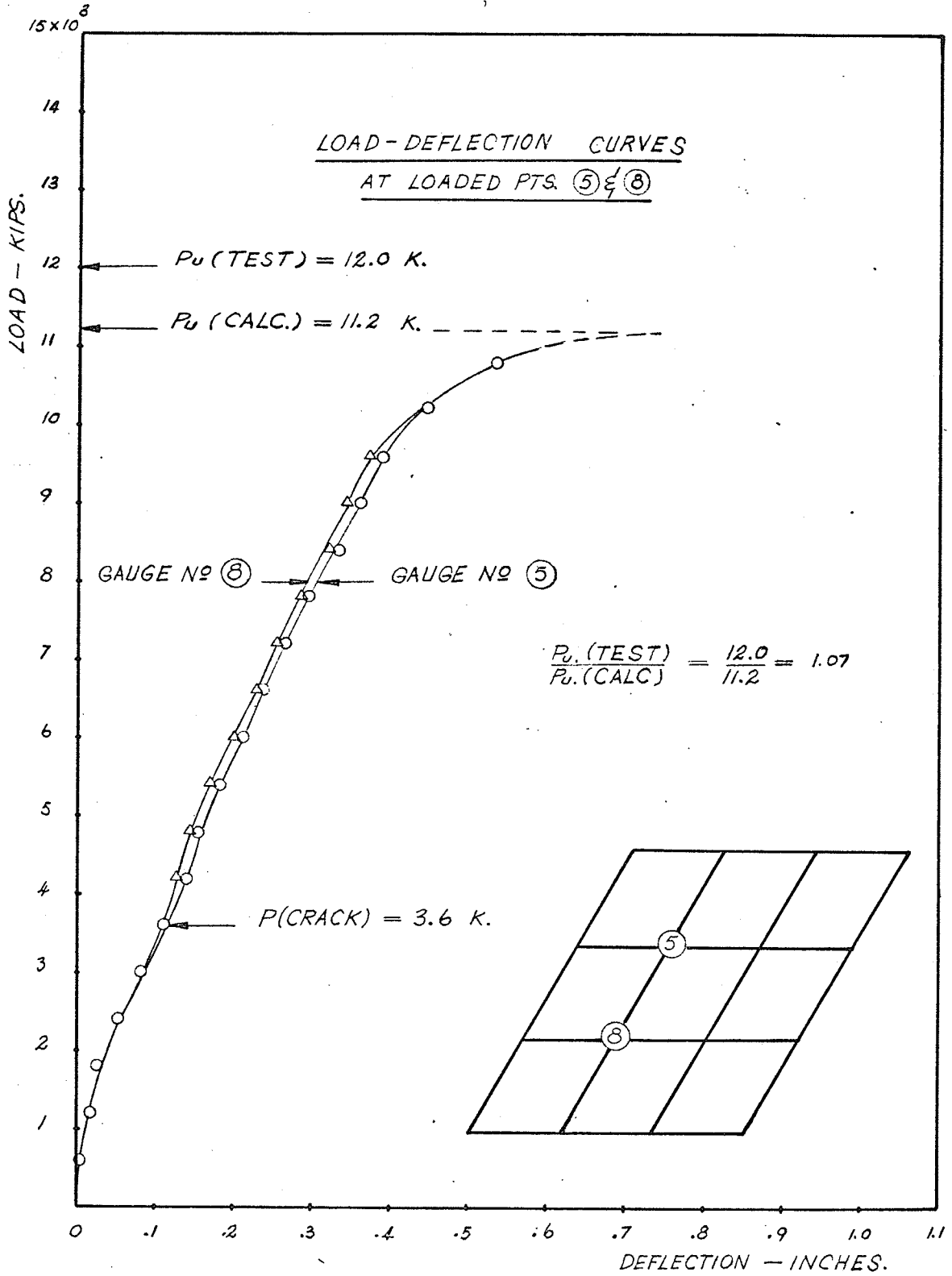


FIGURE. 11 LOAD-DEFLECTION CURVES

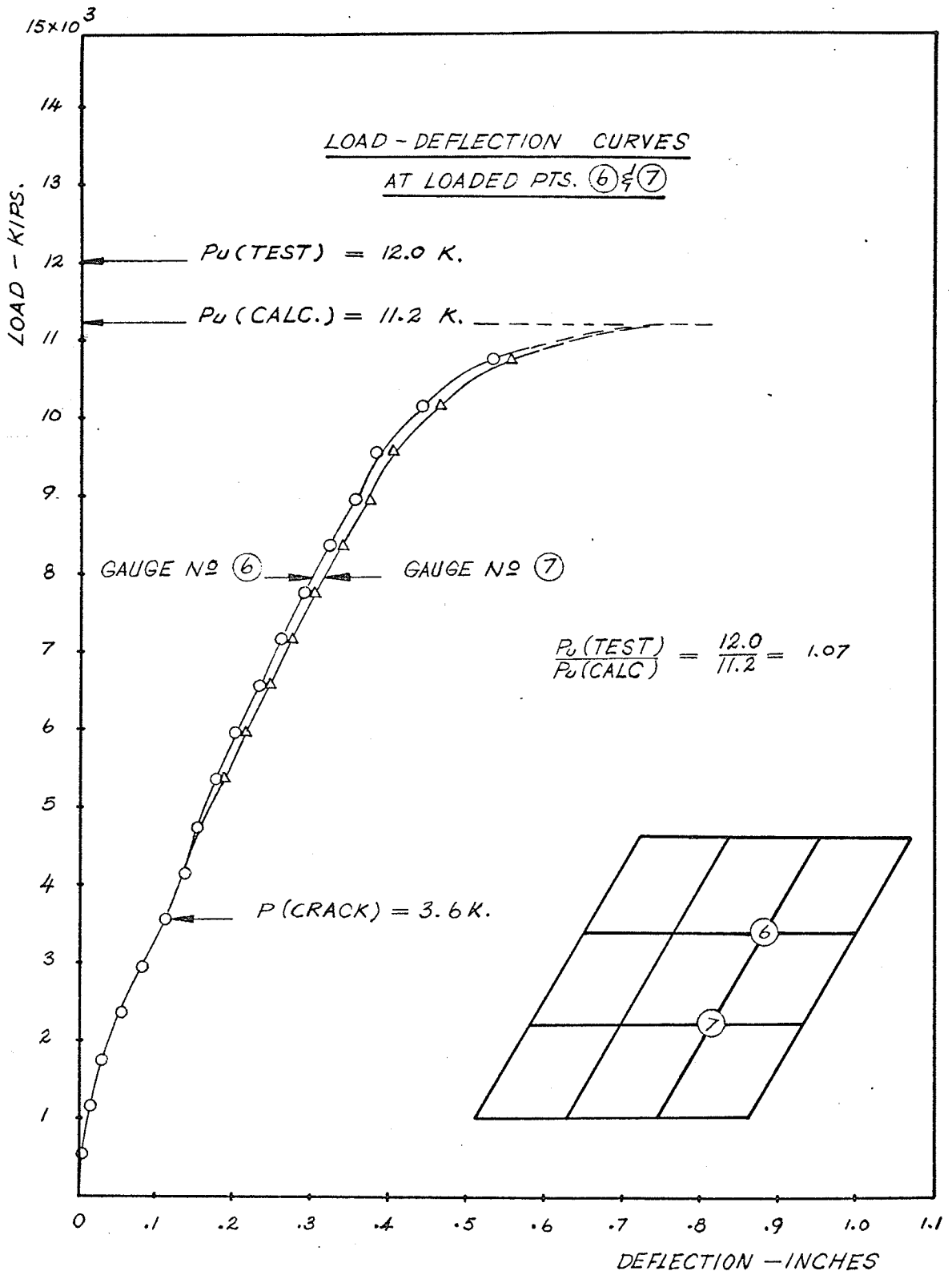


FIGURE. 12 LOAD - DEFLECTION CURVES

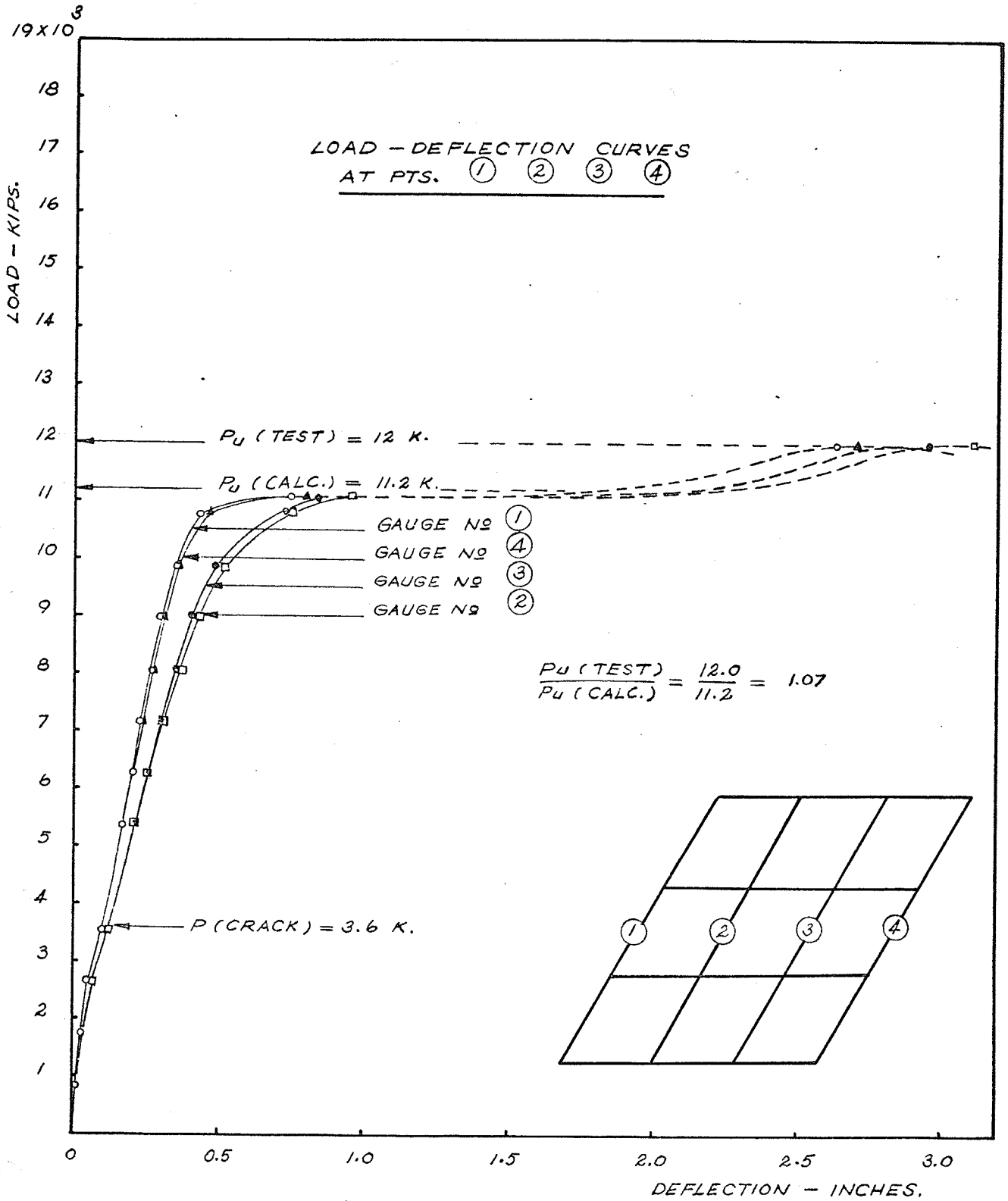


FIGURE. 13 LOAD - DEFLECTION CURVES.

CHAPTER V

CONCLUSIONS AND SUGGESTIONS FOR FURTHER RESEARCH

5.1 Conclusions

From the test results it was shown that the observed mode of collapsed was in agreement with the predicted collapse pattern. Also the ultimate load obtained by equating the external work done by the load during collapse to the work dissipated in the hinges, including torsion, was very close to the predicted value. From the close similarity of both the theoretical and observed strength and the mode of failure, it can be concluded that the test supports the validity of the yield hinge approach of analysis, even where torsion plays a significant part in the collapse.

In fact, there are many methods of analyzing a grillage system. In the past decade many investigators published papers concerned with this matter. Some of the investigators are Jacques Heyman,⁽¹¹⁾ Irving Fader,⁽¹²⁾ Percy J. P.,⁽¹³⁾ Shaw F.S.⁽¹⁴⁾ and Francois N. Ayer.⁽¹⁵⁾ These papers are valuable mathematical tools for the design of such grillage systems, however most of these investigators concentrated on grillages made of open steel sections, where torsional strength is insignificant.

The utilization of the torsional strength is of interest in concrete structures, and in this study the torsional strength was taken into account in the calculations. The pattern of cracks at the hinges which resulted from the bending and torsion are in fairly good agreement with Cowan's Tests.⁽¹⁶⁾ His tests have shown the pattern of cracks for the ratio of $M_B / M_T = 2$ and 2.5. It is apparent that the utilization of torsional strength as in this investigation is on the safe side and these torsional effects should not be neglected in skew structures. Photo 21 and Photo 22 illustrate these pattern of cracks.

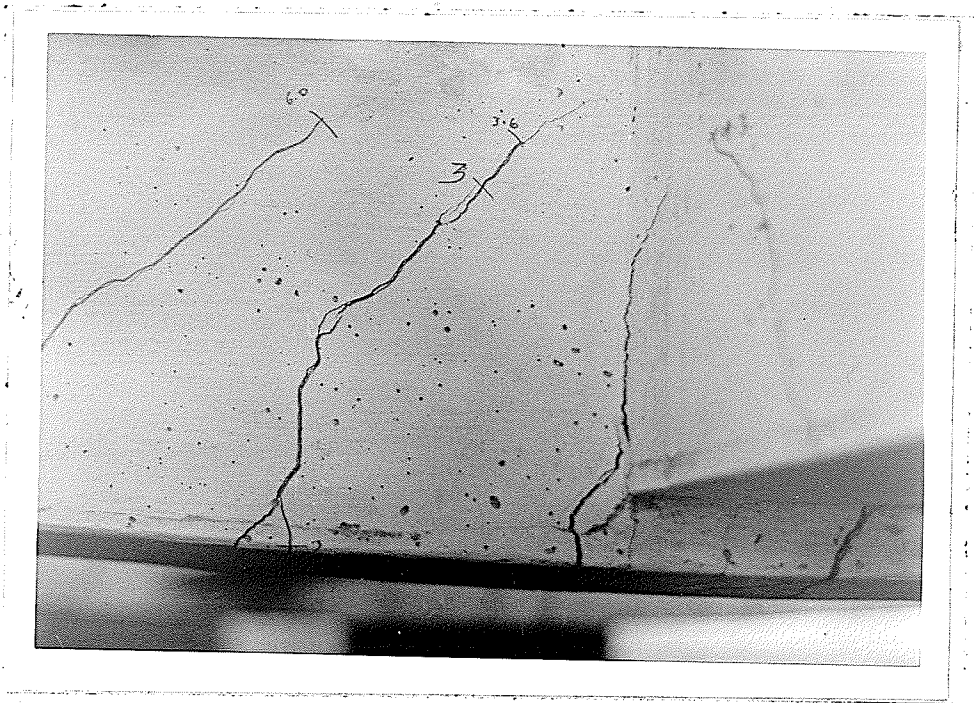


Photo 21 Cracks at the joint

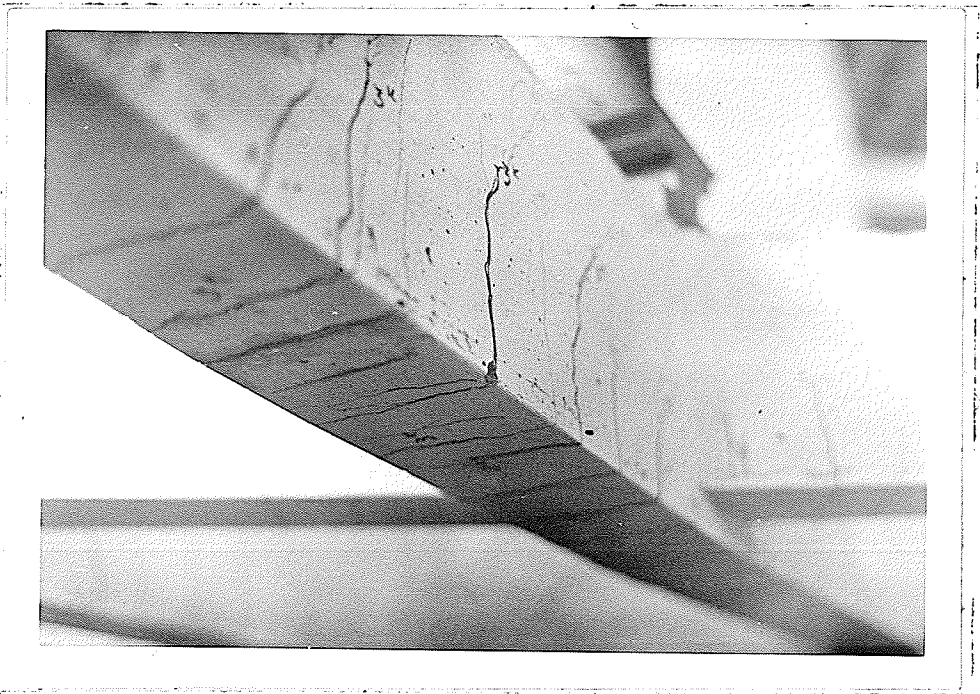


Photo 22 Cracks at the hinge point due to bending and torsion.

The test has also demonstrated that the rotation capacities of the hinges were largely due to ductility of the reinforcing steel, and it was clear that the ductility of hinges was adequate for the full failure mode to develop. The deflections at various points obtained from this test were in good agreement with typical load-deflection curves for reinforced concrete beams. Test curves obtained reveal that after cracks appeared in the concrete on the tension side the curve deviated slightly more for the cracked portion than the uncracked part, due to a reduction in stiffness of the uncracked section. The deflections under two point loads in a free longitudinal beam should be equal in magnitude, but in this test there was a slight difference due to the effects of skew. Because of the asymmetrical restraint offered by the skew transversals, the beam deflections were affected in two ways: (i) a lack of symmetry in the deflections was produced and (ii) the maximum beam deflection was decreased, when compared to that for a simple beam. (17)

5.2 Suggestions for Further Study

The failure pattern of the structure obtained from the test in this study was a simple mode of failure as the collapse occurred across the middle of the structure. This type of failure was induced because of the effect of the high strength of the inner longitudinal and transversal beams. It would be of interest to study the behaviour for the other modes of failure of this type of grillage system. This could be done by making the outer longitudinal beams (or parapet girders) and the end transversal beams a great deal stronger than the inner transversal beams and the diaphragms.

The structure might collapse under the application of the wheel loads with the modes of failure as indicated in the possible modes of failure (modes 2, 3 and 4 in Appendix B. Page 55). These modes of failure utilize the full positive and negative bending strengths of the member as well as torsional strength. The study of the behaviour of the other failure patterns by applying the wheel loads at other points rather than the middle node points is necessary in this field of research. The single point wheel load and double points wheel load applications could yield an interesting mode of failure as well.

Further study for checking the validity of the yield hinges theory with the other complicated shapes of reinforced concrete beams would also be fruitful. The skew reinforced concrete and prestressed concrete grillages of I-sections or Box-sections would also be a useful pursuit.

Finally, a topic which requires a considerable amount of further study is that of shear in grillage systems. The effect of large shear loads on the yielding hinges is of particular importance, especially in structures having short members and supporting heavy loads, as often encountered in bridges.

BIBIOGRAPHY

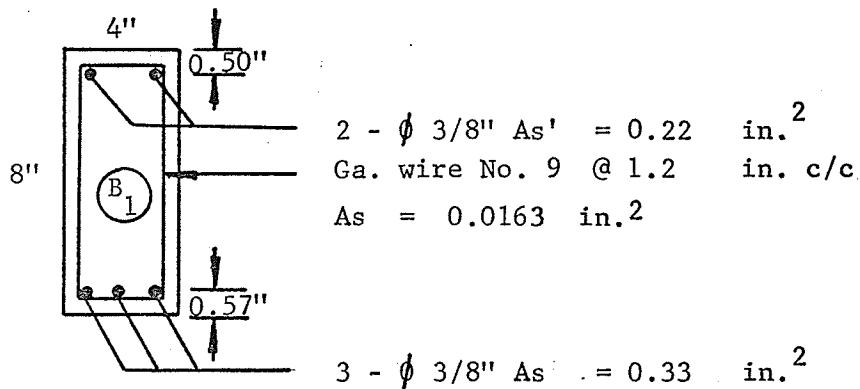
- (1) Charlton, T. M. "Model Analysis of Structures" E & F. N. Spon Limited, London, W. C. 2, 1954.
- (2) Taylor, Thompson & Smulski. "Reinforced - Concrete Bridges". New York: John Wiley & Sons, Inc. London: Chapman & Hall Limited, 1939.
- (3) Scott, W. L. "Reinforced Concrete Bridges". London: Crosby Lockwood & Son Stationers' Hall Court, Ludgate Hill, 1925.
- (4) Reynolds, G. C. "The Strength of Prestressed Concrete Grillage Bridges". Technical Report. Cement and Concrete Association. TRA/268, June 1957.
- (5) Greensberg, H. J. & Prager, W. "Limit Design of Beams and Frames". Proceedings of the American Society of Civil Engineers. Vol. 77, Separate No.59, February 1951. pp.12. Discussion Vol. 78, Separate No. D-59, February 1952, pp. 26 (Ref. of (4)).
- (6) AASHO "The American Association of State Highway Officials - Standard Specifications for Highway Bridges". 1957.
- (7) Phil M. Ferguson "Reinforced Concrete Fundamentals with Emphasis on Ultimate Strength". Second edition, John Wiley & Sons, Inc. 1957.
- (8) Lansdown, A. M. "An Investigation into the Ultimate Behaviour of Reinforced Concrete Beam and Slab Structures, in Particular Bridge Decks". Ph.D. Thesis, 1964.
- (9) ACI Standard "Building Code Requirements for Reinforced Concrete". American Concrete Institute (ACI 318 - 63).
- (10) Concrete Manual United States Department of the Interior Bureau of Reclamation Concrete Manual. "A Manual for the Control of Concrete Construction". Denver, Colorado.

- (11) Jacques Heyman "Inverse Design of Beams and Grillages". Proceedings of the Institution of Civil Engineers. July 1959, Vol. 13, Session 1958-59.
- (12) Irving Fader "Grid Analysis by the Reaction Distribution Method". Journal of the Structural Division. Proceedings of the American Society of Civil Engineers. August 1961, Vol. 87 No. ST6.
- (13) Percy, J. P. "A Design Method for Grillages". Proceedings of the Institution of Civil Engineers, November 1962, Vol. 23.
- (14) Shaw, F. S. "Limit Analysis of Grid Frameworks". Journal of the Structural Division. Proceedings of the American Society of Civil Engineers. October 1963, Vol. 89 No. ST5. Part I.
- (15) Francois N. Ayer & C. Allin Cornell "Grid Moment Maximization by Mathematical Programming". Journal of Structural Division. Proceedings of the American Society of Civil Engineers. February 1968. Vol. 94 No. ST2.
- (16) Henry J. Cowan "Reinforced and Prestressed Concrete in Torsion". London, Edward Arnold (Publishers) Ltd. 1965.
- (17) Nathan M. Newmark, Chester P. Siess & Warren M. Peckham "Studies of Slab and Beam Highway Bridges". Part II. "Tests of Simple-Span Skew I-Beam Bridges" University of Illinois Bulletin Series No. 375, Jan. 12, 1948, No. 31.

APPENDIX A

CALCULATION OF ULTIMATE BENDING STRENGTHS AND TORSIONAL STRENGTHS IN BEAMS.

Calculation of Positive Bending Strengths



$f_y = 66 \text{ ksi}$

$f'_c = 6.062 \text{ ksi}$

$k_1 = 0.75 \text{ (1503ACI)}$

$E_s = 29 \times 10^3 \text{ ksi}$

assume $f_s = f_y$

Calculation of c

$0.33 \times 66 = 0.85 \times 6.062 \times 0.75 \times 4 \times c - 0.85 \times 6.062 \times 0.22$

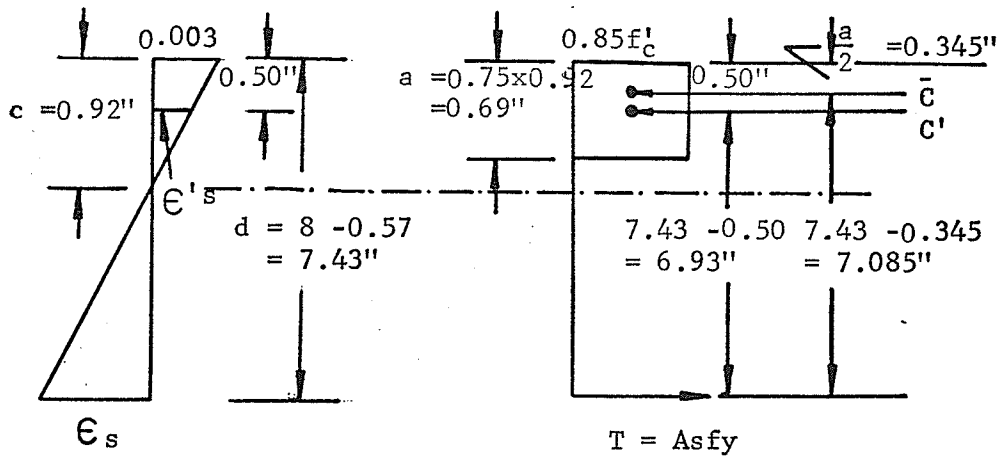
$+ \frac{87}{c} (c - 0.50) 0.22$

$21.8 = 15.45c - 1.133 + 19.13 - \frac{9.57}{c}$

$15.45c^2 - 3.8c - 9.57 = 0$

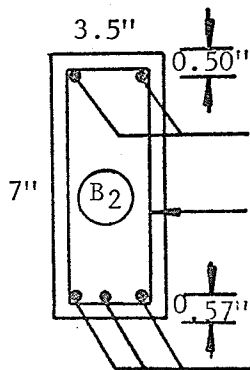
$c = 0.92''$

$$\begin{aligned} \therefore f'_s &= \frac{87}{0.92} (0.92 - 0.50) \\ &= 39.7 < 66 \text{ ksi. OK} \end{aligned}$$



Taking moments of internal forces about the tensile steel.

<u>Conc.</u>	$0.85 \times 6.062 \times 4 \times 0.75 \times 0.92 \times 7.085$	$=$	100	in. - kips
<u>$-A'_s$</u>	$0.85 \times 6.062 \times 0.22 \times 6.93$	$=$	7.85	"
<u>$+A_s$</u>	$39.7 \times 0.22 \times 6.93$	$=$	60.5	
\therefore	M_u	$=$	<u>152.65</u>	in. - kips



$$2 - \phi 3/8'' \text{ As}' = 0.22 \text{ in.}^2$$

$$\text{Ga. wire No. 9 @ 1.5 in. c/c}$$

$$\text{As} = 0.0163 \text{ in.}^2$$

$$3 - \phi 3/8'' \text{ As}' = 0.33 \text{ in.}^2$$

$$\begin{aligned}
 f_y &= 66 \quad \text{ksi.} \\
 f'_c &= 6.062 \quad \text{ksi.} \\
 k_1 &= 0.75 \quad (1503\text{ACI}) \\
 E_s &\doteq 29 \times 10^3 \quad \text{ksi.} \\
 \text{assume } f_s &= f_y
 \end{aligned}$$

Calculation of c .

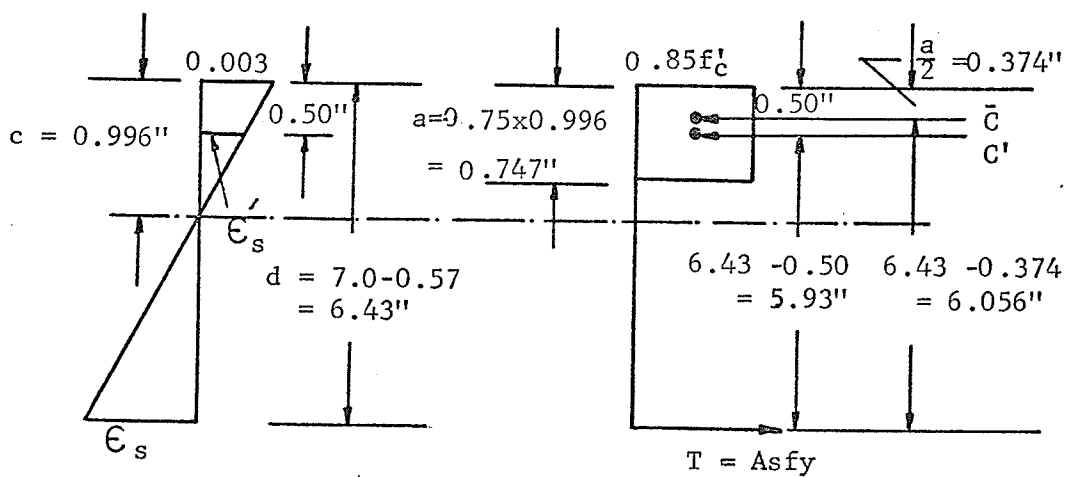
$$\begin{aligned}
 0.33 \times 66 &= 0.85 \times 6.062 \times 0.75 \times 3.5 \times c - 0.85 \times 6.062 \times 0.22 \\
 &\quad + \frac{87}{c} (c - 0.50) 0.22 \\
 21.8 &= 13.5c - 1.133 + 19.3 - \frac{9.57}{c}
 \end{aligned}$$

$$13.5c^2 - 3.8c - 9.57 = 0$$

$$c = 0.996''$$

$$f'_s = \frac{87}{0.996} (0.996 - 0.50)$$

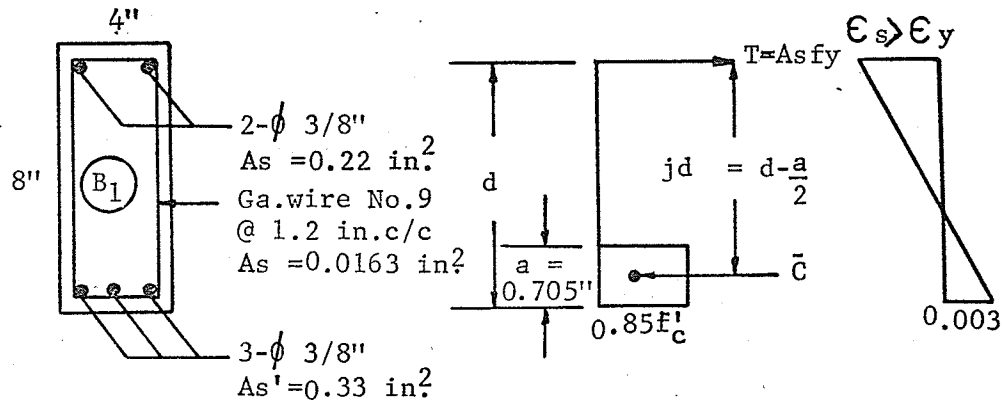
$$= 43.3 < 66 \quad \text{OK}$$



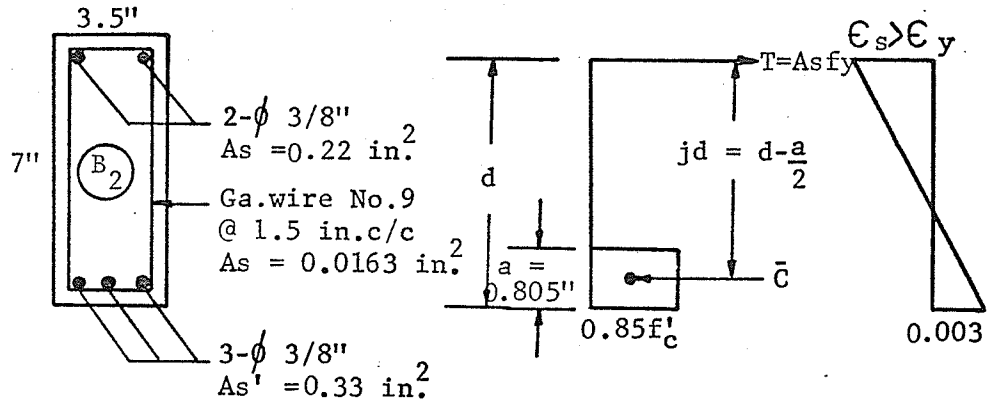
Taking moments of internal forces about the tensile steel.

<u>Conc.</u>	0.85 x 6.062 x 3.5 x 0.747 x 6.056 =	81.5	in. - kips.
<u>-A_s'</u>	0.85 x 6.062 x 0.22 x 5.93 =	- 6.7	"
<u>+A_s'</u>	43.3 x 0.22 x 5.93 =	<u>56.4</u>	"
Mu		<u>131.2</u>	<u>in. - kips.</u>

Calculation of Negative Bending Strengths

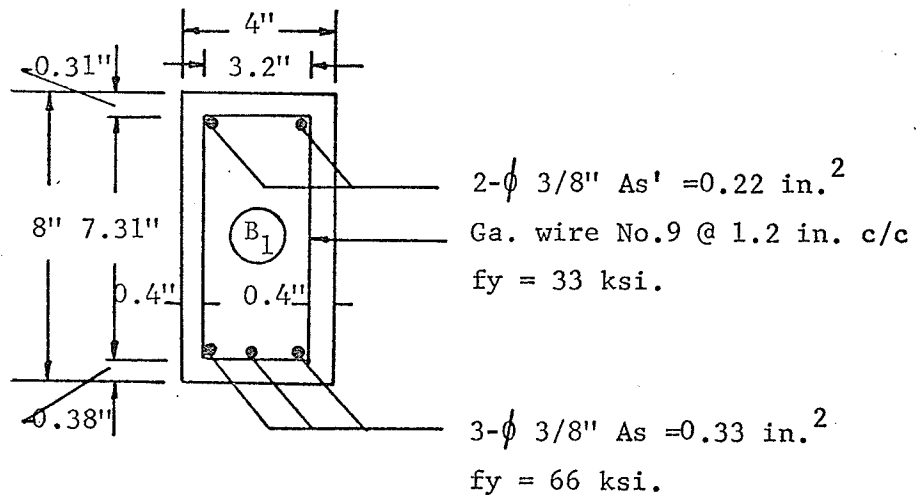


f_y	=	66	ksi.	
f'_c	=	6.062	"	
T	=	C		
$A_s f_y$	=	$0.85 \times f'_c \times a \times b$		
a	=	$\frac{0.22 \times 66}{0.85 \times 6.062 \times 4}$		
	=	0.705"		
M_u'	=	$A_s f_y (jd)$		
	=	$A_s f_y (d - \frac{a}{2})$		
	=	$0.22 \times 66 (7.50 - 0.352)$		
M_u'	=	<u>103.8</u>	in. - kips.	

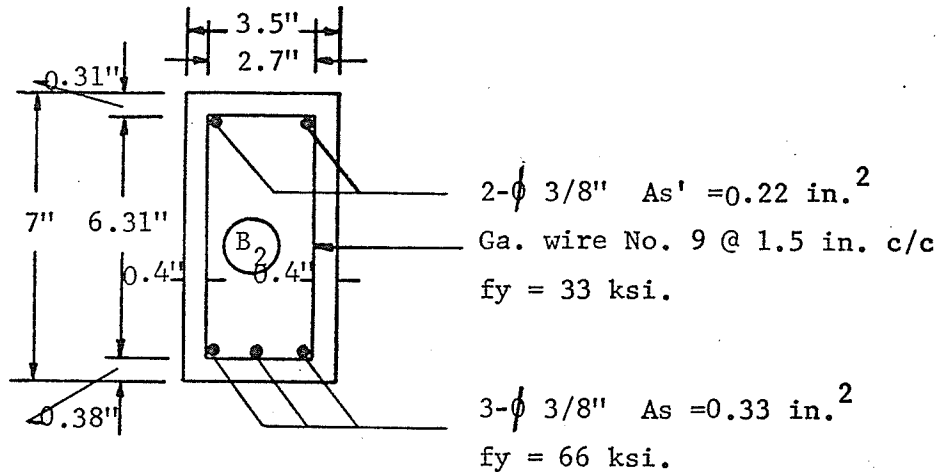


$$\begin{aligned}
 T &= \bar{c} \\
 Asfy &= 0.85 \times f'_c \times a \times b \\
 a &= \frac{0.22 \times 66}{0.85 \times 6.062 \times 3.5} \\
 &= 0.805'' \\
 Mu' &= Asfy(jd) \\
 &= 0.22 \times 66 (6.50 - 0.402) \\
 Mu' &= \underline{88.5 \text{ in. - kips.}}
 \end{aligned}$$

Calculation of Torsional Strengths.



$$\begin{aligned}
 M_T &= \underline{2.356 \text{ A cage. R min (Lansdown}^{(8)})} \\
 F_{yL} &= 66 \text{ ksi.} \\
 F_{yt} &= 33 \text{ ksi.} \\
 b' &= 3.2 \text{ in.} \\
 d' &= 7.31 \text{ in.} \\
 \text{A cage} &= 3.2 \times 7.31 \\
 &= 23.4 \text{ in.}^2 \\
 C &= 2 (b' + d') \\
 &= 2 (3.2 + 7.31) \\
 &= 2 \times 10.51 \\
 &= 21.02 \text{ in.} \\
 p &= 1.2 \text{ in. c/c} \\
 R_L &= n \cdot \frac{F_{yL}}{C} = \frac{5 \times 0.11 \times 66,000}{21.02} \\
 &= 1725 \text{ lb/in.} \\
 R_T &= \frac{F_{yt}}{p} = \frac{0.0163 \times 33,000}{1.2} \\
 &= 448 \text{ lb/in} \\
 \therefore R \text{ min} &= 448 \text{ lb/in} \\
 M_T &= \frac{2.356 \times 23.4 \times 448}{1000} = \underline{24.7 \text{ in - kips.}}
 \end{aligned}$$



$$F_{yL} = 66 \text{ ksi.}$$

$$F_{yt} = 33 \text{ ksi.}$$

$$b' = 2.7 \text{ in.}$$

$$d' = 6.31 \text{ in.}$$

$$A_{\text{cage}} = 2.7 \times 6.31$$

$$= 17 \text{ in.}^2$$

$$C = 2 (b' + d')$$

$$= 2 (2.7 + 6.31)$$

$$P = 2 \times 9.01 = 18 \text{ in.}$$

$$p = 1.5 \text{ in. c/c}$$

$$R_L = n \frac{F_{yL}}{C} = \frac{5 \times 0.11 \times 66,000}{18}$$

$$= 2015 \text{ lb/in.}$$

$$R_T = \frac{F_{yt}}{p} = \frac{0.0163 \times 33,000}{1.5}$$

$$= 358 \text{ lb/in.}$$

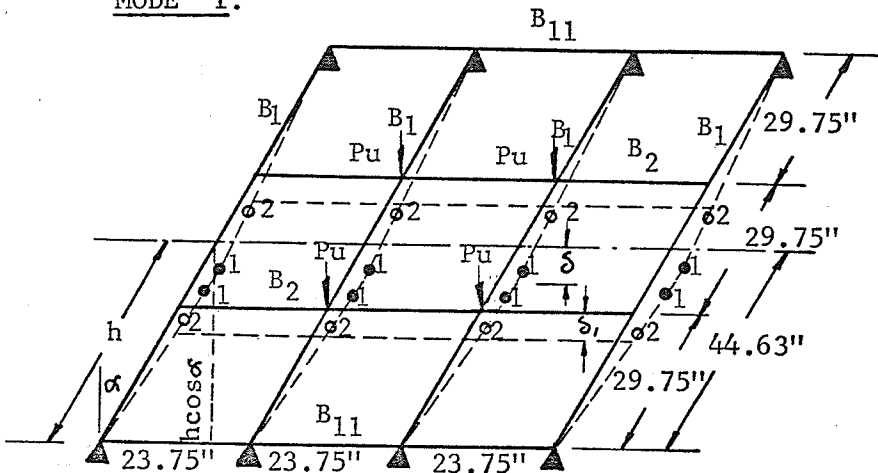
$$\therefore R_{\text{min}} = 358 \text{ lb/in.}$$

$$M_T = \frac{2.356 \times 17 \times 358}{1000} = \underline{14.3 \text{ in. - kips.}}$$

APPENDIX B

CALCULATION OF THE ULTIMATE LOAD FOR THE MODEL

MODE 1.



$$\alpha = 30^\circ$$

$$M_{B1} = 152.65 \text{ in. - kips}$$

$$M_{T1} = 24.7 \text{ "}$$

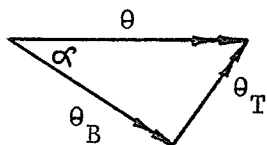
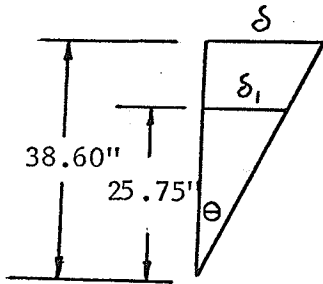
$$h \cos \alpha = 44.63 \times \frac{\sqrt{3}}{2} = 38.60''$$

$$h_1 \cos \alpha = 29.75 \times \frac{\sqrt{3}}{2} = 25.75''$$

$$\delta = 38.6\theta$$

$$\theta = \delta / 38.60$$

$$\delta_1 = \frac{25.75 \delta}{38.60}$$



$$\theta_B = \theta \cos \alpha = \theta \times \cos 30^\circ = 0.866 \theta$$

$$\theta_T = \theta \sin \alpha = \theta \times \sin 30^\circ = 0.50 \theta$$

Item	No.	θ	M_B	M_T	$M\theta$	$nM\theta$
1	8	$0.866 \times \delta / 38.60$	152.65	-	3.42δ	$8 \times 3.42\delta$
2	8	$0.50 \times \delta / 38.60$	-	24.7	0.32δ	$8 \times 0.32\delta$

$$\Sigma nM\theta = 8 \times 3.74 \delta$$

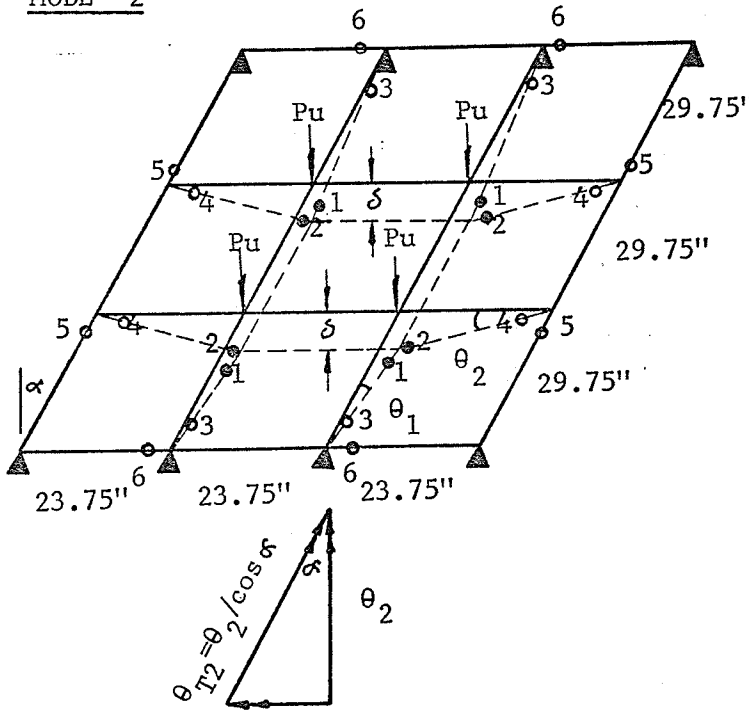
$$W_E = W_D$$

$$4 P \cdot \delta_1 = 8 \times 3.74 \delta$$

$$4 P \times \frac{25.75 \delta}{38.60} = 8 \times 3.74 \delta$$

$$P_u = \frac{8 \times 3.74 \times 38.60}{4 \times 25.75} = \underline{11.20}^K \text{ (lowest)}$$

MODE 2



$$M_{B1} = 152.65 \text{ in. - kips.}$$

$$M_{B2} = 131.20 \text{ "}$$

$$M_{T1} = 24.7 \text{ "}$$

$$M_{T2} = 14.3 \text{ "}$$

$$\theta_1 = \delta / 29.75$$

$$\theta_2 = \delta / 23.75$$

$$\theta_{T1} = \theta_2 \tan 30^\circ = 0.577 \theta_2$$

$$\theta_{T2} = \theta_2 / \cos 30^\circ = 1.153 \theta_2$$

$$\theta_{T1} = \theta_2 \tan \alpha$$

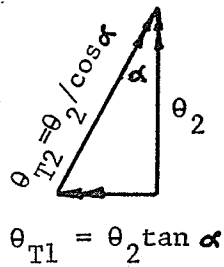
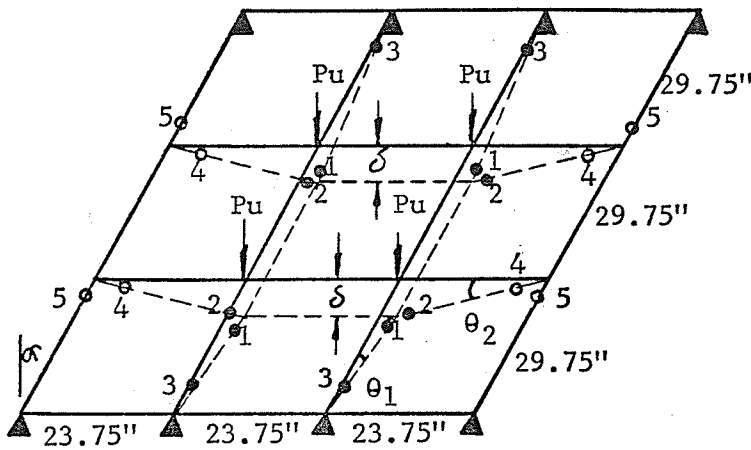
Item	No.	θ	M_B	M_T	$M\theta$	$nM\theta$
1	4	$\delta/29.75$	152.65	-	5.13δ	$4 \times 5.13\delta$
2	4	$\delta/23.75$	131.20	-	5.52δ	$4 \times 5.52\delta$
3	4	$0.577 \delta/29.75$	-	24.7	0.48δ	$4 \times 0.48\delta$
4	4	$0.577 \delta/23.75$	-	14.3	0.347δ	$4 \times 0.347\delta$
5	4	$1.153 \times \delta/29.75$	-	24.7	0.958δ	$4 \times 0.958\delta$
6	4	$1.153 \times \delta/23.75$	-	24.7	1.20δ	$4 \times 1.20\delta$

$$\sum nM\theta = 4 \times 13.64\delta$$

$$Pu = \frac{4 \times 13.64\delta}{4 \times \delta}$$

$$\therefore Pu = \underline{13.64^K}$$

MODE 3



$$\begin{aligned}
 M_{B1} &= 152.65 && \text{in. - kips.} \\
 \bar{M}_{B1} &= 103.80 && \text{"} \\
 M_{B2} &= 131.20 && \text{"} \\
 M_{T1} &= 24.7 && \text{"} \\
 M_{T2} &= 14.3 && \text{"} \\
 \theta_1 &= \delta / 29.75 \\
 \theta_2 &= \delta / 23.75 \\
 \theta_{T1} &= \theta_2 \tan 30^\circ \\
 &= 0.577 \theta_2 \\
 \theta_{T2} &= \theta_2 / \cos 30^\circ \\
 &= 1.153 \theta_2
 \end{aligned}$$

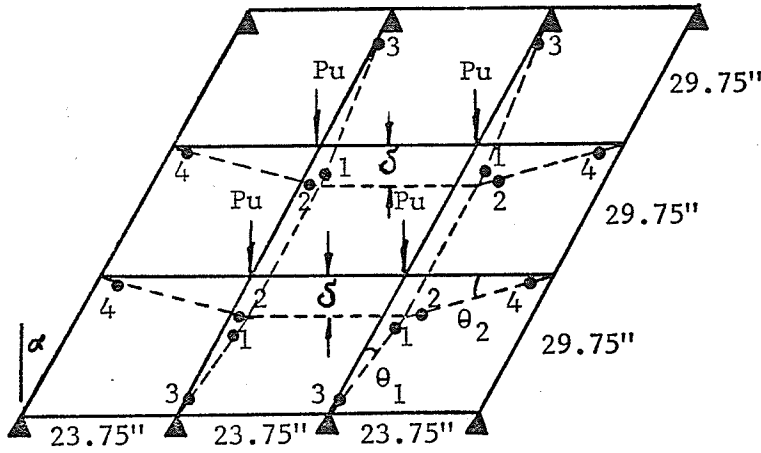
Item	No.	θ	M_B	M_T	$M\theta$	$nM\theta$
1	4	$\delta / 29.75$	152.65	-	5.13δ	$4 \times 5.13 \delta$
2	4	$\delta / 23.75$	131.20	-	5.52δ	$4 \times 5.52 \delta$
3	4	$\delta / 29.75$	103.80	-	3.49δ	$4 \times 3.49 \delta$
4	4	$0.577 \delta / 23.75$	-	14.3	0.347δ	$4 \times 0.347 \delta$
5	4	$1.153 \delta / 23.75$	-	24.7	1.20δ	$4 \times 1.20 \delta$

$$\sum nM\theta = 4 \times 15.69 \delta$$

$$Pu = \frac{4 \times 15.69 \delta}{4 \times \delta}$$

$$\therefore Pu = \underline{15.69^K}$$

MODE 4.



$$\begin{aligned}
 M_{B1} &= 152.65 \text{ in. - kips} \\
 \bar{M}_{B1} &= 103.80 \text{ " } \\
 M_{B2} &= 131.20 \text{ " } \\
 \bar{M}_{B2} &= 88.50 \text{ " } \\
 M_{T1} &= 24.7 \text{ " } \\
 M_{T2} &= 14.3 \text{ " } \\
 \theta_1 &= \delta / 29.75 \text{ " } \\
 \theta_2 &= \delta / 23.75 \text{ " }
 \end{aligned}$$

Item	No.	θ	M_B	M_T	$M\theta$	$nM\theta$
1	4	$\delta / 29.75$	152.65	-	5.13δ	$4 \times 5.13\delta$
2	4	$\delta / 23.75$	131.20	-	5.52δ	$4 \times 5.52\delta$
3	4	$\delta / 29.75$	103.80	-	3.49δ	$4 \times 3.49\delta$
4	4	$\delta / 23.75$	88.50	-	3.72δ	$4 \times 3.72\delta$

$$\sum nM\theta = 4 \times 17.86\delta$$

$$P_u = \frac{4 \times 17.86\delta}{4 \cdot \delta}$$

$$\therefore P_u = \underline{17.86^K}$$

APPENDIX C

TABLES OF LOAD-DEFLECTION READINGS

Gauge readings at points 1, 2, 3 and 4.

No.	Load (lb)	Gauge No.1	Diff.	δ (in.)	Gauge No.2	Diff.	δ (in.)	Gauge No.3	Diff.	δ (in.)	Gauge No.4	Diff.	δ (in.)	Rmks.
1	0	172	0	0	1783	0	0	086	0	0	388	0	0	
2	300	173	001	.001	1784	001	.001	088	002	.002	389	001	.001	* Hair
3	600	174	002	.002	1785	002	.002	091	005	.005	391	003	.003	Cracks
4	900	179	007	.007	1793	010	.010	097	011	.011	396	008	.008	first
5	1200	184	012	.012	1801	018	.018	106	020	.020	403	015	.015	observed
6	1500	189	017	.017	1807	024	.024	113	027	.027	409	021	.021	
7	1800	196	024	.024	1816	033	.033	123	037	.037	416	028	.028	
8	2100	203	031	.031	1825	042	.042	134	048	.048	424	036	.036	
9	2400	217	045	.045	1843	062	.060	152	066	.066	439	051	.051	
10	2700	228	056	.056	1855	072	.072	165	079	.079	450	062	.062	
11	3000	246	074	.074	1874	091	.091	185	099	.099	468	080	.080	
12	3300	258	086	.086	1890	107	.107	200	114	.114	481	093	.093	
13	3600*	273	101	.101	1911	128	.128	218	132	.132	496	108	.108	
14	3900	286	114	.114	1929	146	.146	234	148	.148	509	121	.121	
15	4200	301	129	.129	1943	160	.160	252	166	.166	525	137	.137	

Gauge readings at points 1, 2, 3 and 4. (Continued)

No.	Load (lb)	Gauge No.1	Diff.	δ (in.)	Gauge No.2	Diff.	δ (in.)	Gauge No.3	Diff.	δ (in.)	Gauge No.4	Diff.	δ (in.)	Rmks.
16	4500	-	-	-	-	-	-	-	-	-	-	-	-	** Yield-
17	4800	314	142	.142	1960	177	.177	268	182	.182	537	149	.149	ing of
18	5100	325	153	.153	1975	192	.192	285	199	.199	550	162	.162	the re-
19	5400	337	165	.165	1992	209	.209	300	214	.214	562	174	.174	inforce-
20	5700	349	177	.177	2007	224	.224	316	230	.230	573	185	.185	ment.
21	6000	361	189	.189	2025	242	.242	332	246	.246	585	197	.197	
22	6300	372	200	.200	2040	257	.257	347	261	.261	596	208	.208	
23	6600	384	212	.212	2057	274	.274	364	278	.278	607	219	.219	
24	6900	395	223	.223	2072	289	.289	378	292	.292	618	230	.230	
25	7200	406	234	.234	2088	305	.305	394	308	.308	628	240	.240	
26	7500	419	247	.247	2106	323	.323	412	326	.326	641	253	.253	
27	7800	430	258	.258	2123	340	.340	428	342	.342	651	263	.263	
28	8100	443	271	.271	2158	375	.375	451	365	.365	664	276	.276	
29	8400	455	283	.283	2173	390	.390	468	382	.382	676	288	.288	
30	8700	465	293	.293	2198	415	.415	483	397	.397	686	298	.298	
31	9000	478	306	.306	2215	432	.432	504	418	.418	697	309	.309	
32	9300	488	316	.316	2233	450	.450	520	434	.434	708	320	.320	
33	9600	499	327	.327	2266	483	.483	540	454	.454	721	333	.333	
34	9900	523	351	.351	2303	520	.520	581	495	.495	748	360	.360	
35	10200	545	373	.373	2343	560	.560	618	532	.532	773	385	.385	
36	10500	570	398	.398	2453	670	.670	661	575	.575	800	412	.412	
37	10800	604	432	.432	2538	755	.755	729	643	.643	864	476	.476	
38	11100	-	-	-	-	-	-	-	-	-	-	-	-	

Gauge readings at points 5, 6, 7 and 8.

No.	Load (lb.)	Gauge No.5	Diff.	δ (in.)	Gauge No.6	Diff.	δ (in.)	Gauge No.7	Diff.	δ (in.)	Gauge No.8	Diff.	δ (in.)	Rmks.
1	0	016	0	0	311	0	0	125	0	0	105	0	0	* Hair
2	300	017	001	.001	313	002	.002	127	002	.002	107	002	.002	cracks
3	600	019	003	.003	315	004	.004	129	004	.004	109	004	.004	first
4	900	025	009	.009	320	009	.009	134	009	.009	114	009	.009	observed
5	1200	035	019	.019	328	017	.017	143	018	.018	122	017	.017	
6	1500	037	021	.021	334	023	.023	149	024	.024	127	022	.022	
7	1800	045	029	.029	341	030	.030	156	031	.031	135	030	.030	
8	2100	054	038	.038	351	040	.040	165	040	.040	144	039	.039	
9	2400	070	054	.054	367	056	.056	182	057	.057	158	053	.053	
10	2700	081	065	.065	377	066	.066	194	069	.069	169	064	.064	
11	3000	099	083	.083	394	083	.083	211	086	.086	186	081	.081	
12	3300	112	096	.096	408	097	.097	225	100	.100	200	095	.095	
13	3600*	127	111	.111	422	111	.111	240	115	.115	216	111	.111	
14	3900	140	124	.124	438	127	.127	255	130	.130	232	127	.127	
15	4200	156	140	.140	451	140	.140	271	146	.146	233	128	.128	
16	4500	-	-	-	-	-	-	-	-	-	-	-	-	
17	4800	170	154	.154	463	152	.152	286	161	.161	248	143	.143	
18	5100	184	168	.168	477	166	.166	301	176	.176	261	156	.156	
19	5400	199	183	.183	491	180	.180	315	190	.190	275	170	.170	
20	5700	212	196	.196	504	193	.193	328	203	.203	290	185	.185	

Gauge readings at points 5, 6, 7 and 8. (Continued)

No.	Load (lb.)	Gauge No.5	Diff.	δ (in.)	Gauge No.6	Diff.	δ (in.)	Gauge No.7	Diff.	δ (in.)	Gauge No.8	Diff.	δ (in.)	Rmks.
21	6000	228	212	.212	519	208	.208	343	218	.218	305	200	.200	** Yield-
22	6300	240	224	.224	532	221	.221	356	231	.231	318	213	.213	ing of
23	6600	255	239	.239	547	236	.236	371	246	.246	334	229	.229	the re-
24	6900	269	253	.253	559	248	.248	384	259	.259	347	242	.242	inforce-
25	7200	282	266	.266	573	262	.262	398	273	.273	360	255	.255	ment.
26	7500	299	283	.283	589	278	.278	414	289	.289	376	271	.271	
27	7800	313	297	.297	602	291	.291	428	303	.303	391	286	.286	
28	8100	331	315	.315	622	311	.311	450	325	.325	410	295	.295	
29	8400	347	331	.331	637	326	.326	465	340	.340	426	321	.321	
30	8700	360	344	.344	649	338	.338	479	354	.354	440	335	.335	
31	9000	376	360	.360	670	359	.359	498	373	.373	456	351	.351	
32	9300	390	374	.374	682	371	.371	511	386	.386	470	365	.365	
33	9600	405	389	.389	696	385	.385	527	402	.402	486	381	.381	
34	9900	434	418	.418	726	415	.415	561	436	.436	519	414	.414	
35	10200	462	446	.446	754	443	.443	593	468	.468	552	447	.447	
36	10500	497	481	.481	789	478	.478	630	505	.505	587	482	.482	
37	10800	550	534	.534	848	537	.537	683	558	.558	636	531	.531	
38	11100	**	-	-	-	-	-	-	-	-	-	-	-	

Load-Deflection Readings by Transit Leveling

(After yielding of the reinforcement)

No.	Load (lb.)	Scale Rdg. Pt.1 (in.)	δ (in.)	Scale Rdg. Pt.2 (in.)	δ (in.)	Scale Rdg. Pt.3 (in.)	δ (in.)	Scale Rdg. Pt.4 (in.)	δ (in.)
1	0	1.32	0	1.66	0	1.65	0	1.54	0
2	11100	2.07	0.75	2.62	0.96	2.50	0.85	2.34	0.80
3	12000	3.95	2.63	4.76	3.10	4.60	2.95	4.24	2.70